NASA Contractor Report 3578

The Relative Stress-Corrosion-Cracking Susceptibility of Candidate Aluminum-Lithium Alloys for Aerospace Applications

Patrick P. Pizzo

CONTRACT NAS2-10365
JUNE 1982

NASA

NASA Contractor Report 3578

The Relative Stress-Corrosion-Cracking Susceptibility of Candidate Aluminum-Lithium Alloys for Aerospace Applications

Patrick P. Pizzo
Advanced Research and Applications Corporation
Sunnyvale, California

Prepared for
Ames Research Center
under Contract NAS2-10365

National Aeronautics
and Space Administration

**Scientific and Technical
Information Office**

1982

TABLE OF CONTENTS

ABSTRACT

The results from a two year study of Al-Li-Cu powder metallurgy alloys are summarized in this Final Report on NASA-Ames Contract NAS-10365. Alloys investigated were Al-2.6% Li-1.4% Cu and Al-2.6% Li-1.4% Cu-1.6% Mg. The primary objectives of the study were to 1) identify a practical stress corrosion screening technique, and 2) evaluate the relative stress corrosion crack resistance of the advanced Al-Li alloys. However, much inital effort was involved in characterizing the base properties of the alloys as powder metallurgical processing was found to provide less than anticipated improvement in the tensile ductility and fracture toughness properties, properties which hampered early development of ingot processed Al-Li aerospace alloys and which interfere with isolation of environmental influence in the stress corrosion program. Process, heat treatment, and size/orientational effects on the tensile and fracture behavior were investigated and the results are reported herein. Metallurgical and electrochemical conditions are identified which provide reproducible and controlled parameters for stress corrosion evaluation.

Preliminary stress corrosion test results are reported. In alternate immersion tests, tests which evaluate the combination of crack initiation and crack growth, both Al-Li-Cu alloys appear more susceptible to stress corrosion crack initiation than 7075-T6 aluminum, with the magnesium bearing alloy being the most susceptible. Tests to determine the threshold stress intensity (K_{ISCC}) for the base and magnesium bearing alloys are underway. Twelve each, bolt loaded DCB type specimens are under test (120 days) and limited crack growth in these precracked specimens has been observed. General corrosion in the aqueous sodium chloride environment is thought to be obscuring results through crack tip blunting. Substitute ocean water is being used to minimize general corrosion and pitting in these copper bearing aluminum alloys. Investigation of the stress corrosion crack susceptibility of the two reference alloy continues in an independent study funded through NASA-Ames Research Center.

OVERVIEW

The purpose of this report is to summarize the research that has been completed under NASA-Ames Contract NAS-10365, "The Relative Stress-Corrosion-Cracking Susceptibility of Candidate Aluminum-Lithium Alloys for Aerospace Structural Applications." The contract was initiated in September 1979 and the results herein cover the period September 19, 1979 through September 18, 1981 with emphasis on results completed the last contract period. The first annual report (ARACOR Report:TR-45-1, dated September 1980) documented the tensile properties of the two reference Al-Li-Cu alloys purchased in March 1980. The stress corrosion program was initially envisioned as a three year investigation with the following overall objectives:

1) to identify a practical stress corrosion screening technique for advanced aluminum alloys for aerospace application

2) to evaluate the relative stress corrosion cracking resistance of the two reference Al-Li Cu alloys.

Due to a change in affiliation of the principal investigator, research on Contract NAS-10365 was terminated in September 1981. The stress corrosion experiments in progress were transitioned to an independent stress corrosion evaluation also being funded through the Ames Research Center. A flow diagram for the program as originally conceived is presented on the following page.

There are four sections to this report. Section A is a final and comprehensive compilation of the tensile and fracture properties of the two reference Al-Li-Cu alloys. In Section B, preliminary data concerning the stress corrosion properties of these alloys are presented. In Section C, the mechanical properties of the base and magnesium bearing Al-Li-Cu alloys are compared. The last section, Section D, discusses a time-temperature parametric analysis of the age hardening behavior of the two reference alloys. The material within Sections C and D was presented at the Fall Meeting of TMS-AIME in Louisville, Kentucky in October, 1981.

Stress Corrosion Program
Al-Li-Cu Alloys

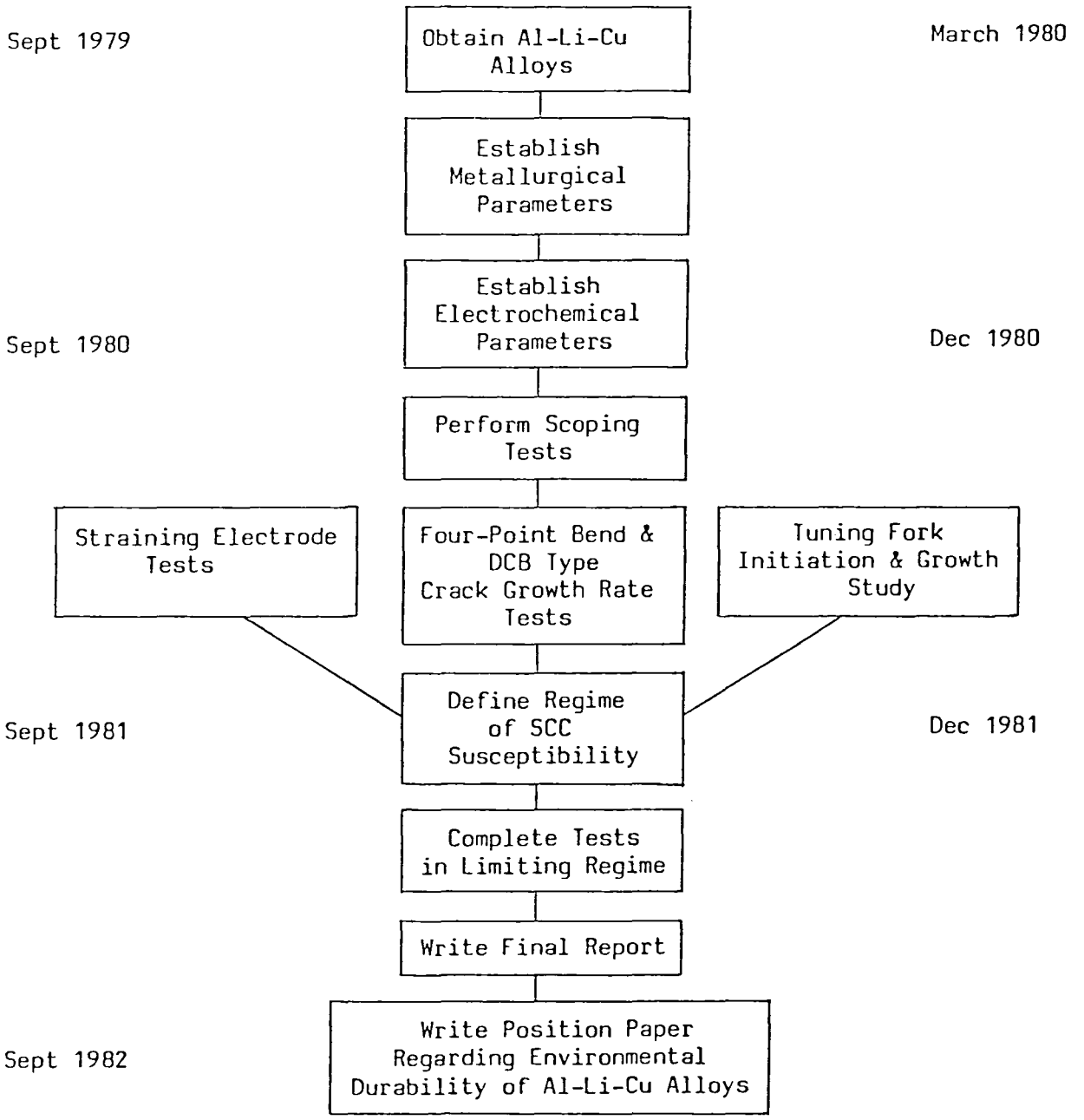

SECTION A

A CHARACTERIZATION OF THE TENSILE AND FRACTURE PROPERTIES OF TWO REFERENCE Al-Li-Cu ALLOYS

LIST OF ILLUSTRATIONS

LIST OF TABLES

INTRODUCTION

In the first annual program report (ARACOR REPORT: TR-45-1 dated September, 1980) the tensile properties of the two reference Al-Li-Cu alloys selected for study were characterized. The available data indicated the following:

(1) Strength properties of approximately 480 MPa yield and 550 MPa ultimate tensile strength, with strain-to-fracture approaching 5%, could be achieved in the A1-Li-Cu alloys.

(2) Reproducibility of the mechanical properties requires close control of both alloy processing and heat treatment steps.

(3) Further testing would be required to demonstrate satisfactory reproducibility of mechanical properties for "control" conditions in the stress corrosion program.

During the current contract period, the required mechanical properties testing has been completed. Data representative of the specimen geometry, process and heat treatment variables pertinent to the stress corrosion study have been obtained. These data are compiled in Tables A3 through A14, a comprehensive tabulation of the tensile properties as a function of aging condition. In addition, fracture toughness test results are reported in Tables A15 and A16. These data are required to interpret the stress corrosion crack growth behavior. Figures A1 through A6 present graphical analyses of the tensile properties reported in Tables A3 through A14. Key parameters which influence the strength and ductility of the A1-Li-Cu alloys for a given aging condition are identified. For reference purposes, the chemical content of the two reference alloys is reported in Table A1; key physical properties are presented in Table A2.

EXPERIMENTAL TECHNIQUE

The aluminum-lithium-copper alloys were purchased from Kawecki-Berylco Industries, Inc., Reading, Pennsylvania. The alloys were processed using powder metallurgy (P/M) techniques. Powders were produced by rapid cooling an atomized molten stream of the target composition in an inert gas (Ar) atmosphere. High purity (0.9999 weight percent) aluminum and a 20 wt. pct. lithium master alloy were combined so as to yield an approximate 2.6 wt. pct. aluminum-lithium melt. High purity element additions were made to adjust the melt to the desired alloy composition. The cooling rate of the atomization process was estimated to be 10^3 K/sec. The resulting powders were spherical, about 150μm in diameter (sized to 100 mesh).

Powders were packed in 6061 aluminum cans (13.7 cm O.D. with 0.32 cm wall), degassed, then cold isostatic pressed to 415 MPa. The compacted powders were then hot upset at 755K against a blind die and extruded at 672K through a 55.9 mm by 14.7 mm (2.2 inch by 0.58 inch) die. This yields an approximate 10:1 extrusion ratio. The chemical compositions of the resulting alloys are presented in Table A1. The lithium content was determined using the wet chemical technique. The zirconium is added to refine grain size and to retard grain growth. Note that the impurity content for elements such as oxygen, calcium, sodium and potassium are very low. The nominal composition of the base alloy is Al-2.6%Li-1.4%Cu: that of the magnesium bearing alloy is Al-2.6%Li-1.4% Cu-1.6% Mg.

Tensile tests were performed using three specimen types: (1) tensile coupon (2) straining electrode specimen and (3) tensile round. These are standard rectangular (types 1 and 2) and round section (type 3), reduced gage, tensile specimens as reported in the first annual report. The tensile coupons

were fabricated from either hot-rolled strip or from the as-extruded plate. The load axis was oriented parallel to the extrusion (or rolling) direction. The straining electrode specimens are also tensile coupons, and are so termed because they are tested in the slow strain rate stress corrosion tests under conditions of constant electrochemical potential. Straining electrode specimens are fabricated from the as-extruded material and they too are oriented so that the load axis is parallel to the extrusion direction. Data from 6.25 mm diameter tensile rounds are also reported. Specimens again represent the as-extruded plate. However, both longitudinal and transverse orientations (with respect to the extrusion direction) are represented in these data. Specific dimensions are indicated for each specimen type in the respective Tables, A3 thru A14.

Solution heat treatment was performed in air prior to specimen fabrication, and material was directly quenched in ice brine at about 278K (5°C). Aging was subsequently performed in a forced air circulation oven maintained to $\pm$ 2K of the desired temperature. Coupon specimens were rough-polished to 600 grit abrasive paper prior to testing. Tensile tests were performed using a closed loop electrohydraulic test system under stroke control. Tensile tests were conducted in accordance with ASTM E8 in ambient air and at a plastic strain rate of 1.4×10^{-4} s^{-1} measured at the 0.2 % strain off-set. Modulus determinations were made from the output of two strain gages attached to opposite sides of tensile coupons (Type (1) specimens). An extensometer was used to determine engineering strain, e, to final fracture. To strain-to-fracture, e_f, data reported herein are the values of the plastic engineering strain-to-fracture as determined from the displacement versus load record.

Fracture toughness tests were also performed. Testing was performed in ambient air in accordance with ASTM E 399-74,

and 12.7 mm thick by 25.4 mm wide compact tension specimens were tested. T-L oriented compact tension specimens were fabricated from the as-extruded plate (i.e., the crack plane normal is parallel to the long-transverse direction, and the crack propagation direction is parallel to the extrusion direction). Fracture toughness data which meet ASTM E399-74 requirements for valid K_{IC} determination are so indicated in the respective tables, A15 and A16.

RESULTS AND DISCUSSION

The impetus for the development of aluminum-lithium aerospace alloys is the high specific strength and high specific stiffness (i.e., strength and stiffness normalized to density) that can be attained with modest lithium additions. The respective Young's modulus and density values for the Al-Li-Cu alloys of this investigation were empirically determined, and the values are reported in Table A2. From these data, the base Al-Li-Cu alloy is found to exhibit an approximate 25% specific stiffness advantage over commercial Al-Cu aerospace alloys. The magnesium bearing alloy enjoys an approximate 27% specific stiffness advantage.

Tensile Properties

The comprehensive tensile data of Tables A3 thru A14 provide a means of assessing the influence of the following variables on tensile properties: (1) specimen geometry, (2) process history (hot rolled vs. as-extruded) (3) solution heat treatment temperature, and (4) aging condition. Those variables which appear to have definite influence on the tensile properties (yield stress, ultimate tensile stress, and strain-to-fracture) of the Al-Li-Cu alloys are summarized in Figures A1 through A6.

The effect of the solution heat treatment temperature on the tensile properties of Al-Li-Cu is illustrated in Fig. A1. Aging curves are presented for as-extruded material aged at 463K (190°C) and 443K (170°C). The vertical limit lines of Fig. A1 are not statistical error bars; the limit lines define the extent of the data scatter. Data for three specimen geometries were included in the analysis. There is much scatter in both yield and ultimate tensile strength at the higher aging temperature; however, there is no dominant trend with respect to the solution heat treatment temperature. However, for 443K

(170°C) aging, the lower solution heat treat temperature, 788K (515°C), produces stronger material for a fixed aging time, particularly for the under-aged material. Note also that the peak ultimate tensile strength is approximately 6% greater for the lower aging temperature irrespective of the solution heat treatment temperature.

The strain-to-fracture, e_f, of the as-extruded Al-Li-Cu alloy is examined as a function of both the solution heat treatment temperature and aging condition in Figure A2. Again two aging temperatures are represented. There is considerable scatter. The scatter can however be correlated with two variables: (1) tensile strength and (2) specimen geometry. The strength/ductility relationship commonly observed in these age hardening systems is evident. Those specimens exhibiting higher strength exhibit lower ductility. In addition, there appears to be a dependence on specimen geometry. The straining electrode specimens are found to exhibit somewhat higher ductility. This is thought to be due to the reduced constraint with respect to slip offered by the small, low abstract ratio, gage section of the straining electrode specimen. The base alloy is found to be strongly textured and the deformation and fracture mechanism active in the phase strengthened alloy involve intensive slip. Due to the reduced constraint, more slip deformation can be accomodated to the point of plastic instability; and increased strain-to-fracture results.

The data of Figures A1 and A2 suggest that optimum mechanical properties for the base Al-Li-Cu alloy are attained for material solution heat treated at 788K (515°C) and slightly overaged at 443K (170°C). Aging times of from 80 to 200 hours are of primary interest. These conditions as well as the peak aged condition (30 to 80 hours at 443K (170°C)) will be investigated in the stress corrosion study.

The effect of the solution heat treatment temperature on the tensile strength of Al-Li-Cu-Mg is presented in Figure A3 for 463K (190°C) aging. Again, the vertical limit lines

indicate the range of scatter of the available data. Trend lines are plotted; tensile data for the three specimen types, fabricated from the as-extruded material, were included in the analysis. The higher solution heat treat temperature, 828K (555°C), clearly results in higher tensile strength irrespective of the time of aging. This is in agreement with preliminary results reported in the first annual report. Yield and tensile strength were monitored for a constant aging time for material solution heat treated at temperatures ranging from 768 K to 828 K (495 to 555°C). These data have been included in Table A12 of this report.

The plastic strain-to-fracture of as-extruded Al-Li-Cu-Mg as a function of solution heat treatment temperature and specimen geometry as presented in Figure A4. The three specimen types (tensile round, straining electrode and tensile coupon) are represented in the data. The open data represent 828K (555°C) solution heat treatment; the closed data, 788K (515°C) treatment. The dashed curve defines the general ductility versus aging time trend curve.

There is much scatter in ductility for a given aging time, and the data are uncorrelated. That is, correlation of the ductility with the solution heat treatment temperature and/or specimen geometry is not apparent. Analysis of the ductility data in combination with the tensile strength trends of Figure A3 establish 828 K(555°C) as the optimum solution heat treatment temperature for the magnesium bearing alloy. The underaged condition is of high interest. The age strengthening of this alloy at 463K (190°) occurs early on. The drop in ductility appears to lag this early strengthening. This underaged regime will be investigated in future study. Attention will also be given the overaged condition. Although results for the tensile

---

See Setion D for results of a study of the early aging response of these Al-Li-Cu alloys.

rounds indicate that ductility may remain low (from 2.5 to 5%) for the overaged magnesium bearing alloy, extensive grain boundary precipitation occurs. And this grain boundary precipitation may have a profound influence on the stress corrosion crack sensitivity. The nature of grain boundary precipitation in the Al-Li-Cu-Mg alloy is illustrated in Section C of this this report.

In the first annual report, a large difference in strength between the as-extruded and hot rolled conditions was noted. A strength decrement of about 9% in terms of both the yield strength (YS) and ultimate tensile strength (UTS) was reported for the hot rolled base alloy. For the magnesium bearing alloy, there is a more pronounced affect; the YS and UTS for the hot rolled material are lower by 42 % and 30% respectively when compared to the as-extruded condition. The subject comparisons are provided in the data of Tables A3 through A14 and are summarized in the trend curves of Figures A5 and A6. The strength decrement associated with hot rolling has been confirmed in duplicate tests. That is the properties of Table A3 and A5 represent material processed independently of that reported in Tables A4 and A6. Specific hot rolling procedures are detailed in the first annual report.

The decrement in strength between the as-extruded and hot rolled conditions is uniform over a broad range of aging conditions (reference Figures A5 and A6). Indeed in the case of the magnesium bearing alloy where data are available, the solution heat treated and quenched condition suffers a similar decrement in strength. It would appear that there is either (1) less solute available for transformation to δ'(and/or θ'), or that (2) precipitation is much more heterogeneous in the hot-rolled material. Specimens to assess the degree of Li (and/or Mg) loss as a result of the hot-rolling process have been analyzed. The lithium content for both the base and the magnesium bearing alloys in the hot rolled condition remains at 2.6 wt. pct.; the

magnesium content of the Al-Li-Cu-Mg is unchanged. Transmission electron microscopy (TEM) of thin film specimens is also in progress and may contribute to an understanding of this anomalous behavior. This phenomenon is further discussed in Section C.

Heretofore, the tensile properties for specimens oriented with their load axis parallel to the extrusion (or rolling) direction were presented. The data of Tables A13 and A14 represent specimens oriented with their load axis parallel to the long transverse direction (perpendicular to the extrusion direction). Limited by the maximum width of the extruded plate, specimen dimensions were adjusted, and the dimensions are noted in the respective tables. When compared to the properties of the longitudinal oriented specimens, the following are observed:

(1) An approximate 10% decrease in UTS, 5% decrease in YS and similar elongation-to-fracture are observed for the base alloy.

(2) An approximate 5% decrease in UTS and YS, and a significant decrease in the elongation-to-fracture, particularly for the peak-aged (26 hour at 463 K) condition occur in the magnesium bearing alloy.

Due to the high extrusion ration (10:1) and to the high degree of texture in these P/M alloys, such results are anticipated.

In addition to tensile strength and ductility, Tables A3 thru A14 report observations concerning discontinuous yielding or the Portevin-Le Chatelier effect. Discontinuous yielding was prevalent in the magnesium bearing alloy particularly for short aging times. The effect was also observed in the base alloy in the hot rolled condition, again for short aging times. The effect is usually attributed to the interaction mobile solute species with dislocation motion during testing. This strain aging phenomenon has been observed in Al-3% Mg alloys

and the 7XXX series aluminum alloys (which contain about 3 percent magnesium). In the case of Al-Li-Cu-Mg, the discontinuous yielding is probably attributable to the presence of magnesium in sold solution. Discontinuous yielding may provide a useful means of investigating the precipitation kinetics of the magnesium bearing Al-Li-Cu alloys. The anomalous early aging response of Al-Li-Cu-Mg is further discussed in Section D of this report.

Fracture Toughness

Characterization of the tensile properties in the first annual report resulted in the following observations regarding ductility of the Al-Li-Cu alloys:

(1) Strain-to-fracture values in excess of 5% would be difficult to attain in either alloy at high strength (YS $\geq$ 450 MPa)

(2) The P/M aluminum-lithium-copper alloys are characterized by limited deformation beyond plastic instability. Very little reduction-in-area is observed and fracture characteristics are brittle.

These observations raised concern for the stress corrosion study in two aspects. One, would there be sufficient and reproducible strain-to-fracture to isolate environmental influence in the slow strain rate crack initiation tests? And secondly, would the fracture toughness of the alloys be sufficient to isolate environmental sensitivity with respect to the threshold stress intensity and crack growth rate under the aqueous 3.5% NaCl environment? The tensile data just presented address the first concern. Fracture toughness data were required to address the second.

Fracture toughness data are presented in Table A15 for the base alloy, and in Table A16 for the magnesium bearing alloy.

Half inch (12.7 mm) thick, one inch (25.4 mm) wide compact tension specimens in the T-L orientation were tested in accordance with ASTM E399-74. Valid K_{IC} values for the requirements of ASTM E399 are so indicated. K_Q values are in close agreement with K_{IC} values for similar aging conditions.

The fracture toughness data for both alloys, irrespective of aging condition, are discouraging. The K_Q values range from 15.8 MPa-$m^{1/2}$ maximum to 7.4 MPa-$m^{1/2}$ minimum. The higher fracture toughness occurs for the underaged condition. As aging proceeds the tensile strength increases and the fracture toughness decreases. The fracture toughness is independent on the solution heat treatment temperature for both alloys. This is somewhat surprising in the case of the Al-Li-Cu-Mg alloy as a correlation between tensile strength and solution heat treatment temperature was indicated in the tensile properties characterization.

The low fracture toughness of the the reference alloys has obvious impact with respect to the stress corrosion program. First, the known threshold value for stress corrosion cracking in the 2XXX series aluminum copper alloys is about equal to the K_{IC} value for the Al-Li-Cu alloys. Thus, K_{ISCC} can only be determined if the reference alloys are very SCC sensitive (i.e., if K_{ISCC} is a very low value). If K_{ISCC} for the Al-Li-Cu alloys is about equal to or greater than 8 MPa-$m^{1/2}$, determination of K_{ISCC} will not be possible. Of course, this would be an indication of reasonable resistance to accelerated crack growth in an aggressive environment. The use of L-T oriented fracture toughness specimens will be employed to increase the ratio of K_{IC} to K_{ISCC}.

Due to the low fracture toughness and limited ductility of the Al-Li-Cu alloys, interpretation of crack initiation phenomenon may also be difficult. Notch sensitivity will be an important consideration in the interpretation of both the slow strain rate tests and the smooth section alternate immersion threshold stress tests.

The low fracture toughness, low tensile ductility and limited reduction-in-area appear to be intrinsic properties of the two reference P/M Al-Li-Cu alloys. Impurities of some concern in Al-Li alloys such as Ca, Na, K are present but at very low levels (reference Table A1). The oxygen content of about 6 ppm is not much different from that found in ingot metallurgy, wrought aluminum products. Preliminary thin film TEM indicate that the solution heat treated, quenched and aged material consists of fine recrystallized grains. The high angle recrystallization grain boundaries are reasonably free of coarse precipitates excepting the overaged Al-Li-Cu-Mg alloy, and very few triple point cavities exist. The role of an extrinsic factor in increasing the notch sensitivity and lowering the fracture toughness of the subject alloys is unsupported. There is obvious need for caution with respect to the development of commercially viable and competitive Al-Li-Cu aerospace alloys via the P/M route as is the case for ingot metallurgy alloys.

SUMMARY

The reference aluminum-lithium-copper P/M alloys do offer the potential of high strength, high modulus and low density. Tensile properties of 460 MPa yield and 550 MPa ultimate tensile strength with strain-to-fracture of 3% are attained in the base alloy. In the magnesium bearing alloy, yield and ultimate tensile strengths of 520 MPa and 600 MPa with about 3.5% strain-to-fracture can be achieved at peak aging. Both alloys enjoy an approximate 25% specific stiffness advantage over competitive Al-Cu aluminum aerospace alloys. The P/M alloys investigated are however characterized by limited deformation beyond plastic instability. Very little reduction in area is observed and fracture characteristics are brittle. Low fracture toughness, a problem that plagued earlier Al-Li commercial alloy development, appears to be an inherent problem in the development of P/M processed Al-Li alloys as well. The limiting fracture toughness for T-L oriented compact tension specimens for both alloys was found to be approximately 8 MPa-$m^{1/2}$ and the fracture toughness was relatively insensitive to the aging condition.

Sufficient mechanical properties data have been generated to characterize the tensile properties of the two reference alloys. The data demonstrate satisfactory reproducibility of properties as required for the stress corrosion evaluation. However, the low fracture toughness of the alloys will have obvious impact on the stress corrosion program. The low fracture toughness will make determination of K_{ISCC} difficult as K_{ISCC} is anticipated to be of the same approximate magnitude as K_Q (or K_{IC}) for S-L oriented DCB type specimens. In addition, the interpretation of SCC initiation data will be difficult. Notch sensitivity and critical flaw size determination will be important considerations in the interpretation of both the slow strain rate tests and the smooth section alternate immersion threshold stress tests.

The low fracture toughness, low tensile ductility and limited reduction in area appear to be intrinsic properties of the Al-Li-Cu alloys. There is obvious need for caution with respect to the development of commercially viable and competitive Al-Li-Cu aerospace alloys via the P/M route as is the case for ingot metallurgy alloys.

CONCLUSIONS

1. Strength properties of 460 MPa yield and 550 MPa ultimate tensile strength with strain-to-fracture of 3% are attained in the base alloy. In the magnesium bearing alloy, yield and ultimate tensile strengths of 520 MPa and 600 MPa respectively with about 3.5% strain-to-fracture can be achieved at peak aging.

2. Both alloys enjoy an approximate 25% specific stiffness advantage over competitive Al-Cu aluminum aerospace alloys.

3. Reproducibility of properties requires close control of both alloy processing and heat treatment. Optimum mechanical properties for the base Al-Li-Cu alloy are attained for as-extruded material solution heat treated at 788 K (515°C) and slightly overaged at 443 K (170°C). For the magnesium bearing alloy, optimum properties are attained for material solution heat treated at 828 K (555°C) and subsequently underaged at 463 K (190°C).

4. A large decrement in tensile strength occurs for Al-Li-Cu alloy hot rolled prior to solution heat treatment and aging when compared to the as-extruded material. For the magnesium bearing alloy the effect is especially pronounced; the yield and the ultimate tensile strength for the hot rolled alloy are 42% and 30% lower respectively, independent of aging time when compared to the as-extruded condition. As lithium and magnesium loss does not occur as a result of the hot rolling process, the strength decrement is attributed to a much more heterogeneous precipitation of the δ' phase. Transmission electron microscopy (TEM) of thin film specimens is in progress and may contribute to an understanding of this anomalous behavior.

5. The P/M aluminum-lithium-copper alloys are characterized by limited deformation beyond plastic instability. Very little reduction-in-area is observed and fracture characteristics are brittle. Low fracture toughness, a problem that plagued earlier commercial alloy development, is predicted to be an inherent problem in the development of P/M processed Al-Li alloys. This is based on an observed fracture toughness of about 8 MPa-$m^{1/2}$ for both alloys in the peak aged condition.

6. The low fracture toughness of the two reference alloys has obvious impact with respect to the stress corrosion program. Determination of K_{ISCC} will be difficult as the value of K_{ISCC} is anticipated to be of the same approximate magnitude as Kq (or K_{IC}). In addition, notch sensitivity will be important in the interpretation of both the slow strain rate tests and the smooth section alternate immersion threshold stress tests.

FIG. A1: THE EFFECT OF SOLUTION HEAT TREATMENT TEMPERATURE ON THE TENSILE PROPERTIES OF Al-Li-Cu

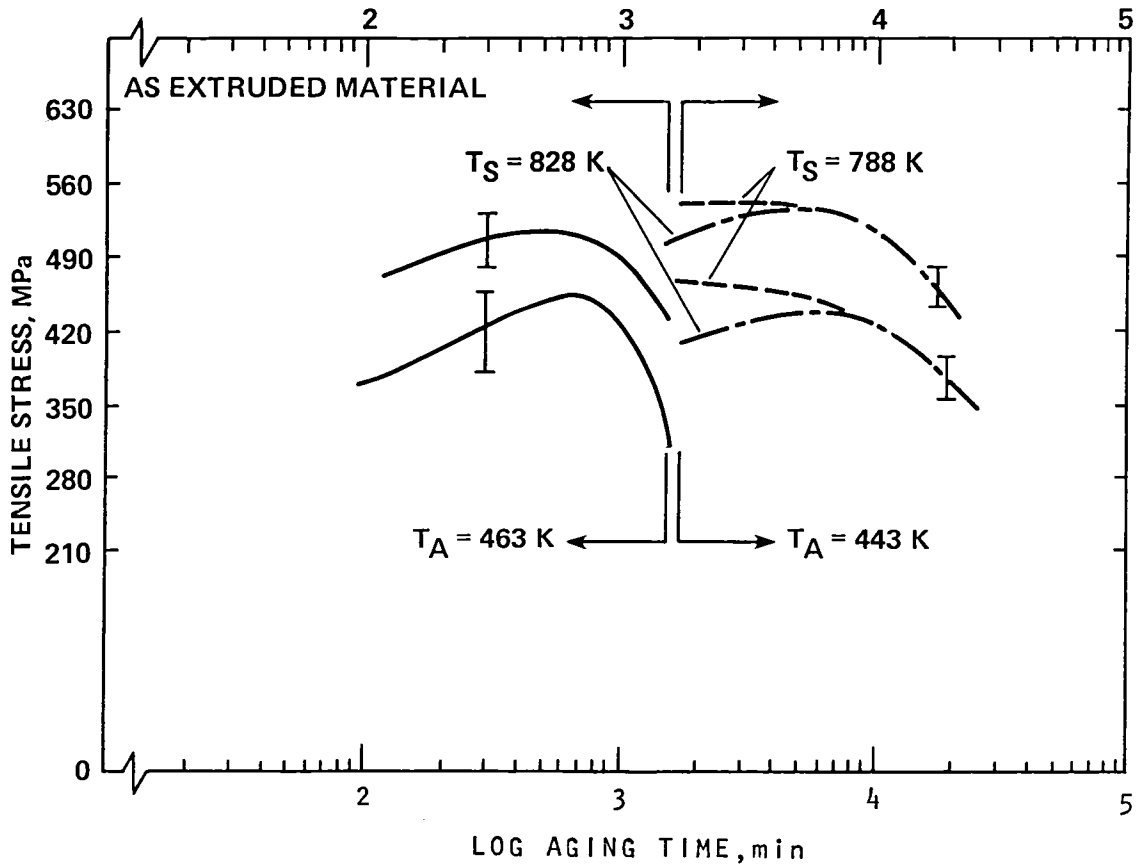

FIG A2: THE STRAIN TO FRACTURE OF Al-Li-Cu AS A FUNCTION OF THE SOLUTION HEAT TREATMENT AND AGING TEMPERATURES

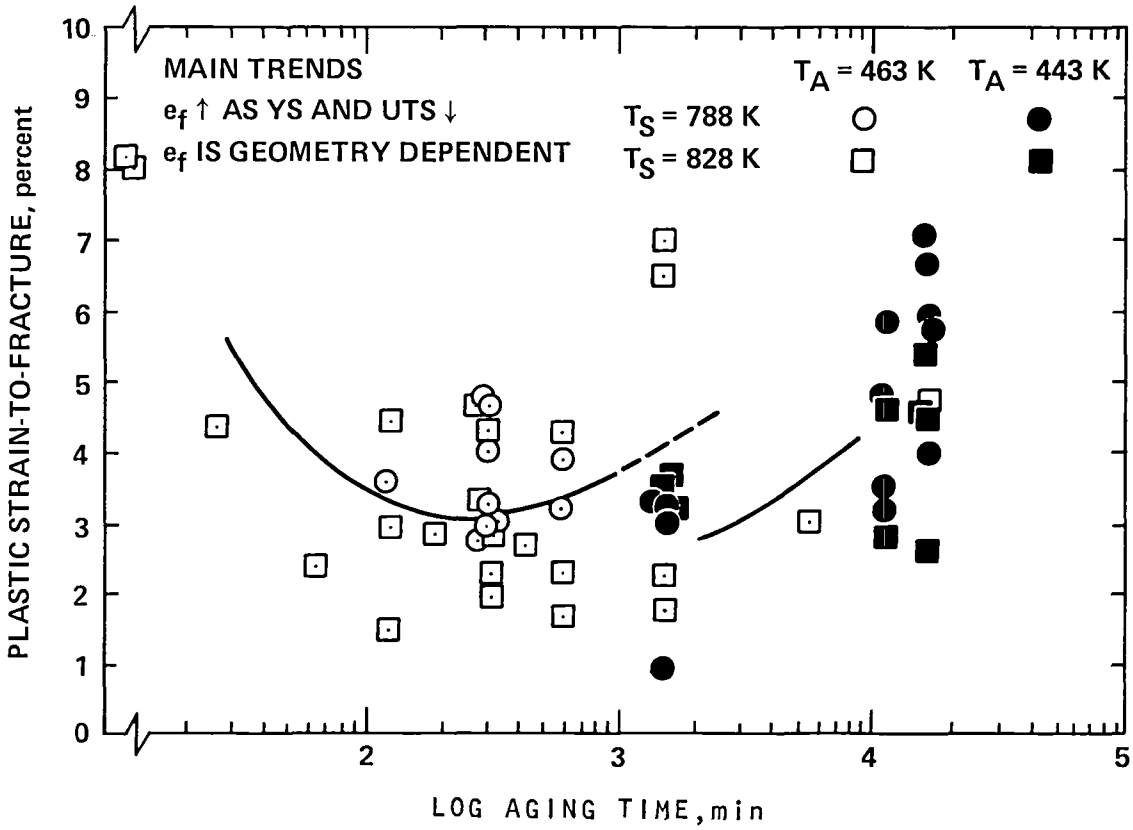

FIG A3: THE EFFECT OF SOLUTION HEAT TREATMENT TEMPERATURE ON THE TENSILE PROPERTIES OF Al-Li-Cu-Mg

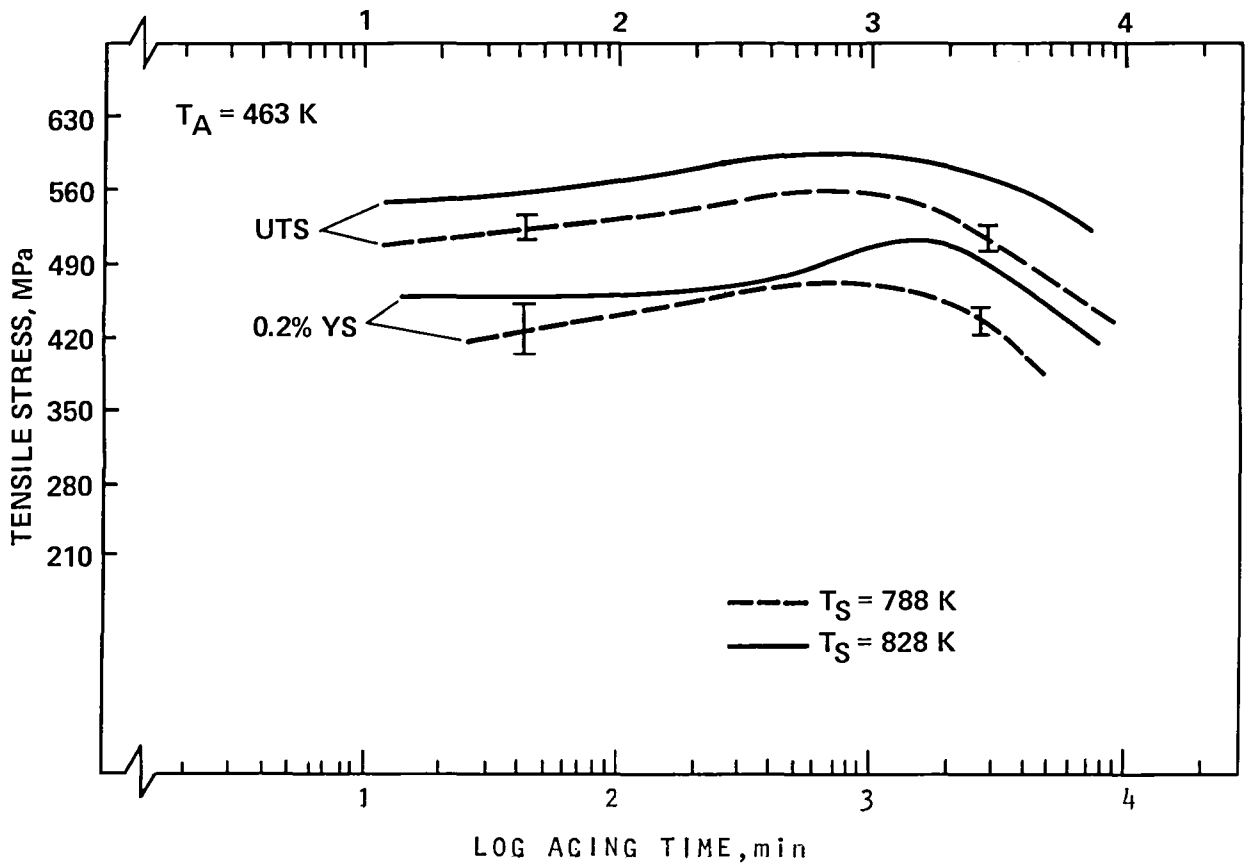

FIG. A4: THE PLASTIC STRAIN-TO-FRACTURE OF AS-EXTRUDED Al-Li-Cu-Mg AS A FUNCTION OF SOLUTION HEAT TREATMENT TEMPERATURE AND SPECIMEN GEOMETRY

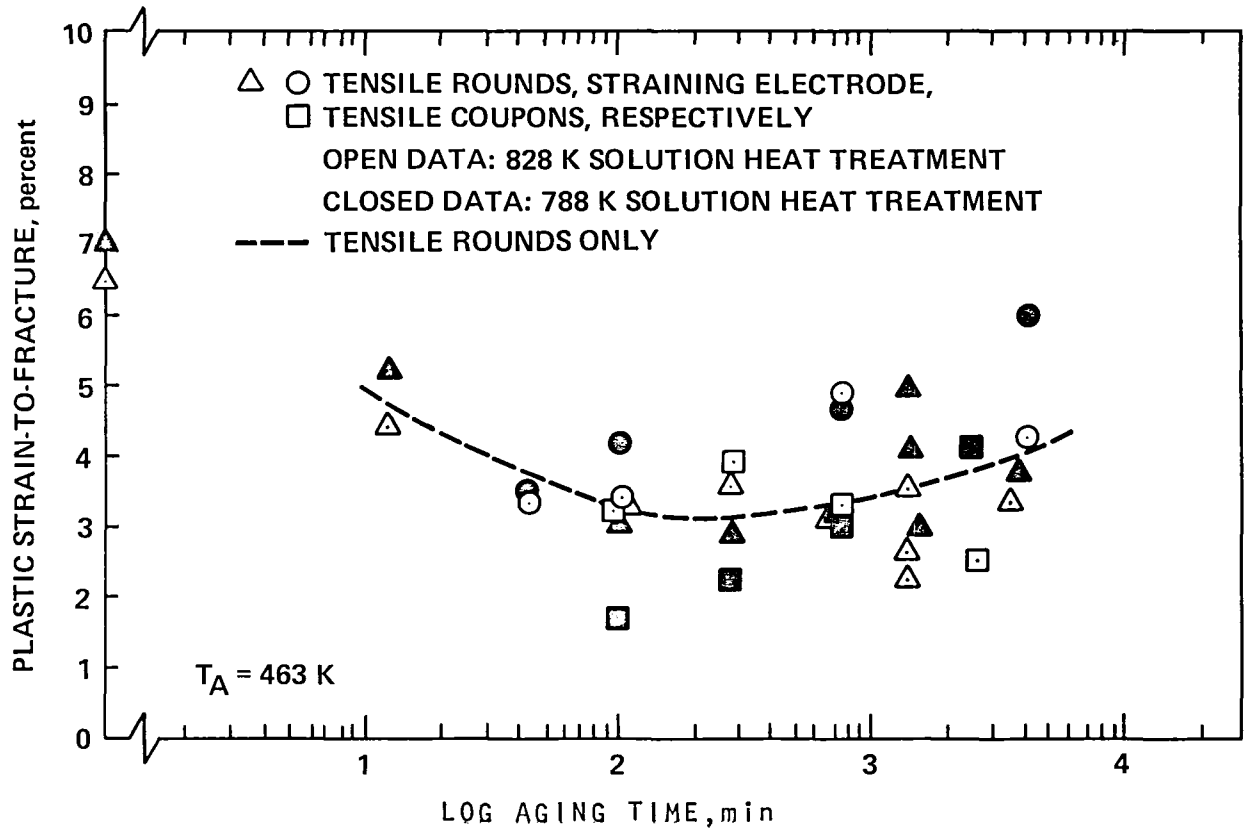

FIG. A5: THE EFFECT OF HOT ROLLING ON THE TENSILE PROPERTIES OF Al-Li-Cu

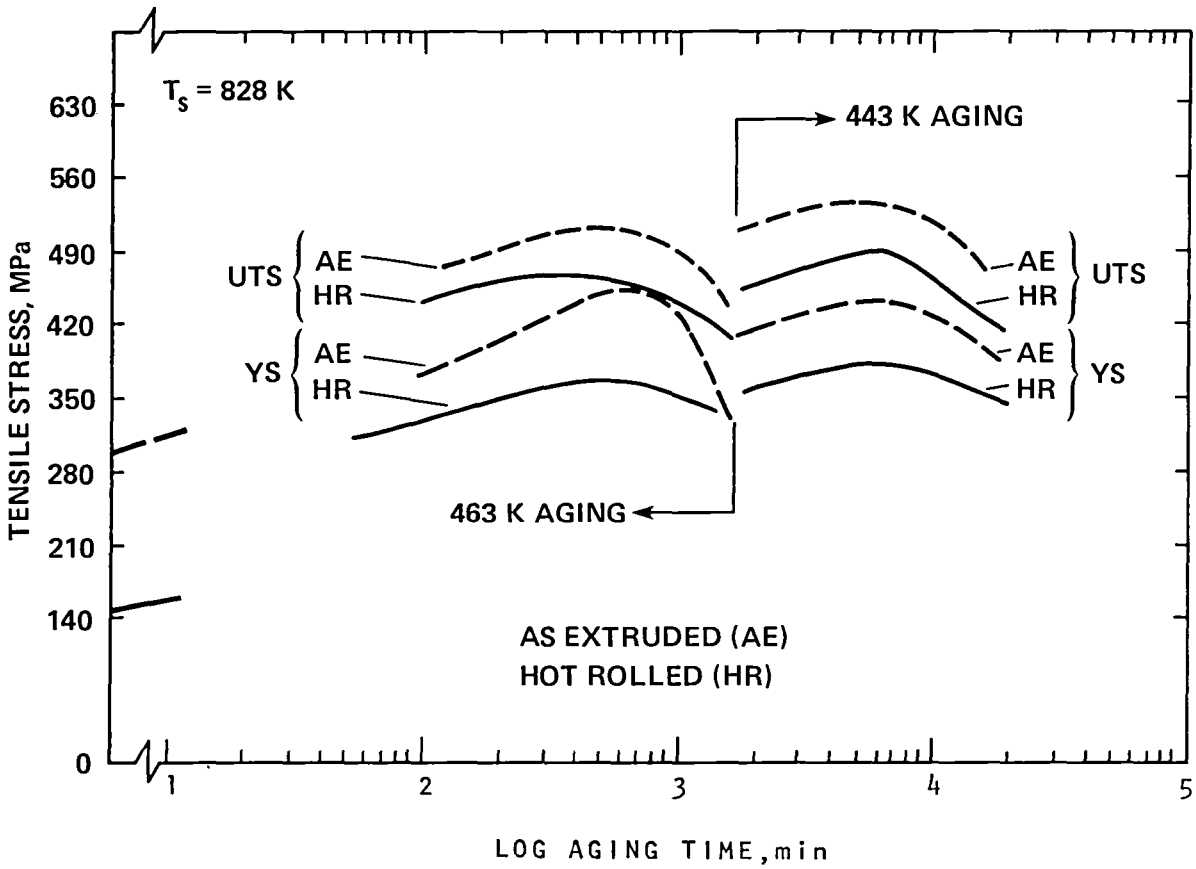

FIG. A6: THE EFFECT OF HOT ROLLING ON THE TENSILE PROPERTIES OF Al-Li-Cu-Mg

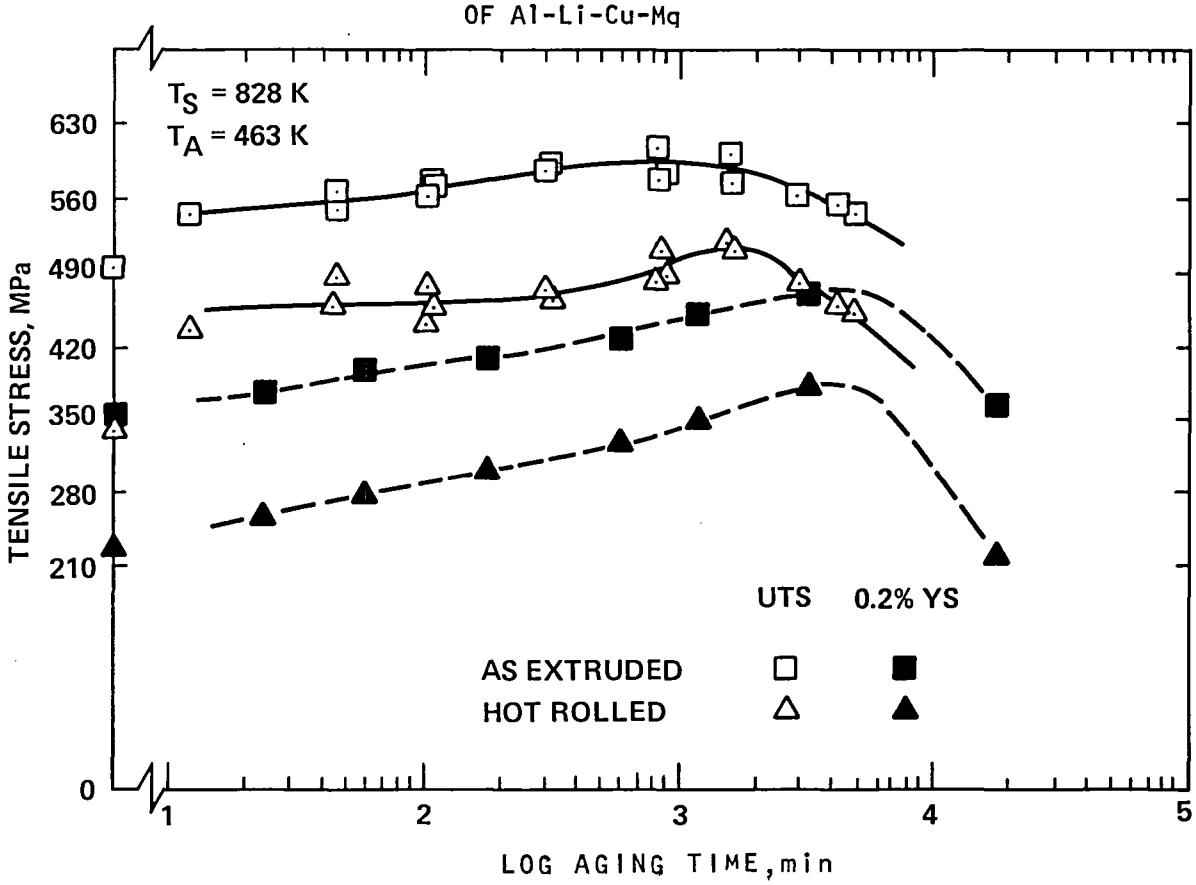

Table A1

Chemical Composition of the Aluminum-Lithium-Copper Alloys

Base Alloy (Al-Li-Cu)	Composition (Wt. Pct)										
	Li	Cu	Mg	Zr	Si	Fe	Mn	Zn	Ti	Cr	Be
	Nominal Alloy Composition										
Mg Bearing (Al-Li-Cu-Mg) Alloy	2.6	1.4	.006	.09	.03	.06	.005	.02	.03	.002	.005
	2.6	1.4	1.6	.09	.03	.05	.005	.02	.03	.002	.005

	Trace Impurities (ppm)			
	O	Ca	Na	K
Base Alloy	6	3	2	1
Mg Bearing Alloy	5	3	1	1

Table A2

Physical Properties of the Base and Magnesium Bearing Alloys

Youngs' Modulus

$E_{(Al\text{-}Li\text{-}Cu)} = 80.0$ GPa

$E_{(Al\text{-}Li\text{-}Cu\text{-}Mg)} = 80.7$ GPa

Density

$P_{(Al\text{-}Li\text{-}Cu)} = 2.55$ gm/cm^3

$P_{(Al\text{-}Li\text{-}Cu\text{-}Mg)} = 2.53$ gm/cm^3

Note: (a) Alloys in the peak aged condition

(b) Modulus determined from the output of two Strain gages on opposite sides of flat tensile coupons

(c) Density measurements: determined experimentally using Archimedes' principle

Table A3

THE TENSILE PROPERTIES OF Al-Li-Cu AS A FUNCTION OF AGING CONDITIONS FOR TENSILE COUPONS FABRICATED FROM HOT ROLLED STRIP AND SOLUTION HEAT TREATED FOR 0.67 HOURS AT 828K[1] - [4]

Specimen Designation	Aging Condition		0.2% Offset Yield Strength		Ultimate Tensile Strength		Slope of Stress/ Strain Curve (GPa)		Plastic Strain-to-fracture
	Time(hrs)	Temp(K)	Ksi	(MPa)	Ksi	(MPa)	@ e = 0.5%	@ e = 2.0%	(%)
71[3][4]	- as SHT -		21.8	(150)	44.7	(308)	4.27	2.48	8.1
72[4]	0.4	443	40.5	(279)	57.2	(394)	3.88	2.17	4.5
73[4]	2.0	443	46.7	(322)	61.5	(424)	6.21	1.70	3.1
74	7.0	443	47.7	(329)	63.6	(439)	6.21	1.85	2.8
75	30.0	443	53.0	(366)	67.3	(464)	6.18	--	2.3
76	100.0	443	57.6	(397)	71.8	(495)	6.23	1.25	3.1
77	300.0	443	51.0	(352)	62.0	(428)	4.48	0.79	4.9
78	1.0	463	48.2	(332)	62.6	(431)	5.34	1.57	2.5
102	2.0	463	49.5	(341)	66.3	(457)	6.18	2.22	4.6
79	5.0	463	51.5	(355)	68.1	(469)	5.87	1.28	4.8
101	10.0	463	54.6	(377)	68.5	(472)	5.23	1.77	4.4
80	30.0	463	49.1	(338)	59.6	(411)	5.12	1.11	1.9

Notes: (1) Tensile coupons nominally 1.7mm thick with a 50mm by 9mm reduced section.

(2) Tests performed in accordance with ASTM E8 in ambient air and at an initial engineering strain rate of $1.4 \times 10^{-4} s^{-1}$.

(3) Flow stress is notably strain independent at low plastic strains (up to 0.4% strain); analogous to yield point phenomenon.

(4) Load/displacement curve is mildly serrated (70N peak-to-peak); more pronounced with increasing strain.

Table A4

THE TENSILE PROPERTIES OF Al-Li-Cu AS A FUNCTION OF AGING CONDITIONS FOR TENSILE COUPONS FABRICATED FROM HOT ROLLED STRIP, SOLUTION HEAT TREATED FOR 0.67 HOURS AT 788K(1) - (2)

Specimen Designation	Aging Condition		0.2% Offset Yield Strength		Ultimate Tensile Strength		Slope of Stress/ Strain Curve (GPa)		Plastic Strain-to-fracture
	Time(hrs)	Temp(K)	Ksi	(MPa)	Ksi	(MPa)	@ e = 0.5%	@ e = 2.0%	(%)
252	200.0	443	51.3	(354)	61.9	(427)	4.90	1.22	3.6
253	200.0	443	52.4	(361)	61.6	(424)	4.74	1.07	3.2
254	5.0	463	48.0	(331)	61.1	(421)	6.37	1.67	3.1
255	5.0	463	47.2	(325)	60.6	(418)	6.49	1.85	2.9

Notes: (1) Tensile coupons nominally 1.6mm thick with a 25mm by 4.8mm reduced section.

(2) Tests performed in accordance with ASTM E8 in ambient air and at an initial engineering strain rate of $1.4 \times 10^{-4} s^{-1}$.

Table A5

THE TENSILE PROPERTIES OF Al-Li-Cu-Mg AS A FUNCTION OF AGING CONDITIONS FOR TENSILE COUPONS FABRICATED FROM HOT ROLLED STRIP AND SOLUTION HEAT TREATED FOR 0.67 HOURS AT 828K[1] - [5]

Specimen Designation	Aging Condition		0.2% Offset Yield Strength		Ultimate Tensile Strength		Slope of Stress/ Strain Curve (GPa)		Plastic Strain-to-fracture
	Time(hrs)	Temp(K)	Ksi	(MPa)	Ksi	(MPa)	@ e = 0.5%	@ e = 2.0%	(%)
81[3]	- as SHT -		33.4	(230)	51.5	(355)	3.36	1.41	12.9
82[3]	0.4	463	38.2	(264)	55.5	(382)	3.70	1.19	11.8
106[3]	1.0	463	40.8	(282)	58.3	(402)	3.92	1.52	11.3
83[4]	3.0	463	44.4	(306)	59.5	(410)	4.16	1.29	6.5
84[4]	10.0	463	48.0	(331)	62.4	(431)	4.03	1.22	6.4
105	20.0	463	51.3	(354)	65.8	(454)	4.28	1.86	6.8
85	55.0	463	56.5	(390)	68.7	(474)	5.10	1.23	2.3
86[5]	300	463	33.2	(230)	53.0	(365)	7.44	1.57	5.1
87[4]	30	443	44.5	(307)	56.5	(390)	4.04	1.24	3.4
88	300	443	55.0	(379)	67.1	(463)	3.49	1.26	2.7
89	1000	443	56.1	(387)	68.6	(473)	4.15	1.54	3.6
90	1000	443	57.1	(393)	66.1	(456)	4.06	1.45	2.1

Notes: (1) Tensile coupons nominally 1.7mm thick with a 50mm by 9mm reduced section.

(2) Tests performed in accordance with ASTM E8 in ambient air and at an initial engineering strain rate of $1.4 \times 10^{-4} s^{-1}$.

(3) Load/displacement curve is strongly serrated (130N peak-to-peak); more pronounced with increasing strain.

(4) Load/displacement curve is mildly serrated (90N peak-to-peak); more pronounced with increasing strain.

(5) Specimen exhibited load drop prior to final fracture.

Table A6

THE TENSILE PROPERTIES OF Al-Li-Cu-Mg AS A FUNCTION OF AGING CONDITIONS FOR TENSILE COUPONS FABRICATED FROM HOT ROLLED STRIP, SOLUTION HEAT TREATED FOR 0.67 HOURS AT 788K[1] - [3]

Specimen Designation	Aging Condition		0.2% Offset Yield Strength		Ultimate Tensile Strength		Slope of Stress/ Strain Curve (GPa)		Plastic Strain-to-fracture
	Time(hrs)	Temp(K)	Ksi	(MPa)	Ksi	(MPa)	@ e = 0.5%	@ e = 2.0%	(%)
258[3]	10.0	463	45.5	(314)	61.2	(422)	6.54	1.83	5.2
259[3]	10.0	463	43.2	(298)	58.8	(405)	6.56	1.89	3.9
260	55.0	463	46.8	(323)	61.4	(424)	5.56	1.94	3.1
261	55.0	463	52.5	(362)	63.4	(437)	5.39	1.53	3.2

Notes: (1) Tensile coupons nominally 1.6mm thick with a 25mm by 4.8mm reduced section.

(2) Tests performed in accordance with ASTM E8 in ambient air and at an initial engineering strain rate of $1.4 \times 10^{-4} s^{-1}$.

(3) Load/displacement curve mildly serrated (70N peak-to-peak) beyond 1.5% plastic strain.

Table A7

THE TENSILE PROPERTIES OF Al-Li-Cu AS A FUNCTION OF AGING CONDITIONS FOR TENSILE COUPONS FABRICATED FROM THE AS-EXTRUDED PLATE AND SOLUTION HEAT TREATED 1.0 HOUR AT 828K (1) - (3)

Specimen Designation	Aging Condition		0.2% Offset Yield Strength		Ultimate Tensile Strength		Slope of Stress/ Strain Curve (GPa)		Plastic Strain-to-fracture
	Time(hrs)	Temp(K)	Ksi	(MPa)	Ksi	(MPa)	@ e = 0.5%	@ e = 2.0%	(%)
145	2	463	59.5	(410)	69.3	(478)	5.39	(3)	1.6
146	5	463	59.2	(408)	73.8	(509)	6.36	2.09	3.0
147	10	463	67.6	(466)	74.2	(512)	3.67	(3)	1.8

Notes: (1) Tensile coupons nominally 1.7mm thick with a 50mm by 9mm reduced section.

(2) Tests performed in accordance with ASTM E8 in ambient air and at an initial engineering strain rate of $1.4 \times 10^{-4} s^{-1}$.

(3) Insufficient strain-to-fracture to obtain data.

Table A8

THE TENSILE PROPERTIES OF Al-Li-Cu-Mg AS A FUNCTION OF SOLUTION HEAT TREATMENT AND AGING CONDITIONS FOR TENSILE COUPONS FABRICATED FROM THE AS-EXTRUDED PLATE(1) - (3)

Specimen Designation	Aging Condition		0.2% Offset Yield Strength		Ultimate Tensile Strength		Slope of Stress/ Strain Curve (GPa)		Plastic Strain-to-fracture
	Time(hrs)	Temp(K)	Ksi	(MPa)	Ksi	(MPa)	@ e = 0.5%	@ e = 2.0%	(%)
			Solution heat teated for 1 hour at 788K						
155(3)	1.75	463	72.1	(497)	79.6	(549)	0.44	1.36	2.4
152(3)	5.0	463	74.2	(512)	81.8	(564)	1.92	1.03	2.3
153	14.0	463	70.9	(489)	81.4	(561)	4.23	1.66	3.1
154	48.0	463	63.3	(436)	76.0	(524)	5.35	1.53	4.2
			Solution heat treated for 1 hour at 828K						
151	1.75	463	67.5	(465)	82.8	(571)	5.36	2.56	3.4
148	5.0	463	68.4	(472)	85.4	(589)	5.92	2.54	4.0
149	14.0	463	71.2	(491)	84.4	(582)	5.63	2.16	3.4
150	48.0	463	70.2	(484)	82.1	(566)	4.58	1.59	2.6

Notes: (1) Tensile coupons nominally 1.7mm thick with a 50mm by 9mm reduced section.

(2) Tests performed in accordance with ASTM E8 in ambient air and at an initial engineering strain rate of $1.4 \times 10^{-4} s^{-1}$.

(3) The flow stress is notably strain independent at low plastic strains. In addition, serrated flow is observed (178N peak-to-peak) beyond 0.5% strain.

Table A9

THE TENSILE PROPERTIES OF Al-Li-Cu AS A FUNCTION OF SOLUTION HEAT TREATMENT AND AGING CONDITIONS FOR STRAINING ELECTRODE SPECIMENS FABRICATED FROM THE AS-EXTRUDED PLATE[1], [3]

Specimen Designation	Aging Condition		0.2% Offset Yield Strength		Ultimate Tensile Strength		Slope of Stress/ Strain Curve (GPa)		Plastic Strain-to-fracture
	Time(hrs)	Temp(K)	Ksi	(MPa)	Ksi	(MPa)	@ e = 0.5%	@ e = 2.0%	(%)
			Solution heat treated for 1 hour at 788K						
133	2.0	463	54.0	(372)	69.9	(482)	5.94	0.90	3.7
130	5.0	463	57.0	(393)	72.6	(501)	5.62	0.90	4.2
129	5.0	463	56.2	(387)	72.5	(500)	6.62	0.83	4.9
134	5.0	463	56.3	(388)	73.0	(503)	6.39	0.80	4.8
135[3]	10.0	463	66.7	(460)	75.5	(520)	3.75	0.54	3.3
131[3]	199	443	58.3	(402)	70.4	(486)	5.21	1.08	5.9
132[3]	295	443	55.3	(381)	67.4	(465)	5.03	1.19	6.8
136[3]	300	443	53.5	(369)	64.8	(447)	3.56	0.53	5.8
			Solution heat treated for 1 hour at 828K						
41	3.0	463	60.6	(418)	70.6	(487)	3.48	1.68	3.0
126	5.0	463	53.9	(372)	71.5	(493)	6.63	0.97	4.4
125[3]	5.0	463	55.7	(384)	70.8	(488)	6.75	0.81	3.4
42[3]	26.0	463	46.3	(319)	61.0	(421)	5.17	1.85	6.6
43[3]	26.0	463	48.5	(335)	63.5	(438)	5.00	1.76	7.1
127	199	443	58.1	(401)	71.8	(495)	5.78	1.48	4.7
128	295	443	55.7	(384)	68.4	(471)	5.78	1.48	4.6

Notes: (1) Straining electrode specimens nominally 1.4mm thick with a 25mm by 4.8mm reduced section.

(2) Tests performed in accordance with ASTM E8 in ambient air and at an initial engineering strain rate of $1.4 \times 10^{-4}\ s^{-1}$

(3) Specimen exhibited load drop prior to final fracture.

Table A10

THE TENSILE PROPERTIES OF Al-Li-Cu-Mg AS A FUNCTION OF SOLUTION HEAT TREATMENT AND AGING CONDITIONS FOR STRAINING ELECTRODE SPECIMENS FABRICATED FROM THE AS-EXTRUDED PLATE[1]-[5]

Specimen Designation	Aging Condition		0.2% Offset Yield Strength		Ultimate Tensile Strength		Slope of Stress/ Strain Curve (GPa)		Plastic Strain-to-fracture
	Time(hrs)	Temp(K)	Ksi	(MPa)	Ksi	(MPa)	@ e = 0.5%	@ e = 2.0%	(%)
			Solution heat treated for 1 hour at 788K						
142[4]	0.75	463	65.4	(451)	78.6	(542)	4.67	0.72	3.6
143[5]	1.75	463	62.1	(428)	78.4	(541)	5.47	0.92	4.3
141	14.0	463	67.7	(467)	81.2	(560)	4.86	0.74	4.8
144	80	463	56.8	(392)	70.7	(487)	6.01	0.59	6.1
			Solution heat treated for 1 hour at 828K						
138[3][4]	0.75	463	71.5	(493)	82.6	(570)	1.32	0.61	3.5
139[5]	1.75	463	70.2	(484)	84.3	(581)	4.13	0.85	3.5
137	14.0	463	74.8	(516)	89.0	(613)	4.19	0.73	5.0
140	80	463	66.1	(456)	80.0	(552)	5.62	0.65	4.4

Notes: (1) Straining electrode specimens nominally 1.4mm thick with a 25mm by 4.8mm reduced section.

(2) Tests performed in accordance with ASTM E8 in ambient air and at an initial engineering strain rate of $1.4 \times 10^{-4}\ s^{-1}$.

(3) Flow stress is notably strain independent at low plastic strains; analogous to yield point phenomenon. In addition, serrated flow is observed (133N peak-to-peak) beyond 0.5% strain.

(4) Load/displacement curve strongly serrated (133N peak-to-peak).

(5) Load/displacement curve mildly serrated (70N peak-to-peak) beyond 2.5% plastic strain.

Table A11

THE TENSILE PROPERTIES OF Al-Li-Cu AS A FUNCTION OF SOLUTION HEAT TREATMENT AND AGING CONDITIONS FOR TENSILE ROUNDS FABRICATED FROM THE AS-EXTRUDED PLATE[1]-[3]

Specimen Designation	Aging Condition Time(hrs)	Temp(K)	0.2% Offset Yield Strength Ksi	(MPa)	Ultimate Tensile Strength Ksi	(MPa)	Slope of Stress/ Strain Curve (GPa) @ e = 0.5%	@ e = 2.0%	Plastic Strain-to-fracture (%)
			Solution heat treated at 768K						
62	26	443	61.6	(425)	75.5	(521)	5.70	1.97	3.4
			Solution heat treated at 788K						
61	26	443	70.0	(483)	80.0	(552)	4.45	1.54	3.1
159	26	443	68.9	(475)	74.7	(515)	4.41	(4)	1.1
64	26	443	69.5	(479)	80.1	(552)	4.43	1.50	3.3
115	199	443	58.0	(400)	70.7	(488)	4.84	1.45	4.9
116	295	443	55.9	(385)	67.3	(464)	4.82	0.90	7.2
114	300	443	56.0	(386)	66.7	(460)	4.65	0.41	6.0
160	300	443	57.3	(395)	70.5	(486)	4.97	1.38	4.1
113	5	463	58.9	(406)	72.8	(502)	6.17	0.81	3.1
161	5	463	55.8	(385)	72.2	(498)	6.95	2.72	3.4
162	10	463	57.1	(394)	73.2	(505)	6.56	2.10	4.0
			Solution heat treated at 808K						
60	26	443	58.7	(404)	75.9	(523)	6.72	2.24	3.1

Table A11 (continued)

THE TENSILE PROPERTIES OF Al-Li-Cu AS A FUNCTION OF SOLUTION HEAT TREATMENT AND AGING CONDITIONS FOR TENSILE ROUNDS FABRICATED FROM THE AS-EXTRUDED PLATE(1)-(3)

Specimen Designation	Aging Condition Time(hrs)	Aging Condition Temp(K)	0.2% Offset Yield Strength Ksi	0.2% Offset Yield Strength (MPa)	Ultimate Tensile Strength Ksi	Ultimate Tensile Strength (MPa)	Slope of Stress/Strain Curve (GPa) @ e = 0.5%	Slope of Stress/Strain Curve (GPa) @ e = 2.0%	Plastic Strain-to-fracture (%)
			Solution heat treated at 828K						
59	26	443	57.2	(394)	74.6	(514)	6.69	2.25	3.5
163	26	443	61.0	(421)	75.5	(521)	6.47	2.05	3.6
111	199	443	61.8	(426)	73.1	(504)	4.41	1.54	2.9
112	295	443	56.8	(391)	67.1	(463)	4.90	1.32	2.7
110	300	443	56.0	(386)	67.8	(467)	4.91	0.53	4.6
164	300	443	55.0	(379)	66.7	(460)	4.77	1.43	5.5
109	5	463	62.4	(431)	73.7	(508)	5.54	0.77	2.4
165	5	463	66.7	(460)	75.6	(521)	4.05	1.73	2.1
166	10	463	65.5	(452)	74.2	(512)	4.07	1.57	2.4

Notes: (1) Tensile round specimens nominally 32mm gage length with a 6.25mm diameter section.

(2) Tests performed in accordance with ASTM-E8 in ambient air and at an initial engineering strain rate of 1.4×10^{-4} S^{-1}

(3) Specimens 59, 60, 61 and 62 solution heat treated for 0.67 hours. All others held 1 hour prior to cold water quench.

(4) Insufficient strain-to-fracture to obtain data.

Table A12

THE TENSILE PROPERTIES OF Al-Li-Cu-Mg AS A FUNCTION OF SOLUTION HEAT TREATMENT AND AGING CONDITIONS FOR TENSILE ROUNDS FABRICATED FROM THE AS-EXTRUDED PLATE[1]-[7]

Specimen Designation	Aging Condition		0.2% Offset Yield Strength		Ultimate Tensile Strength		Slope of Stress/ Strain Curve (GPa)		Plastic Strain-to-fracture
	Time(hrs)	Temp(K)	Ksi	(MPa)	Ksi	(MPa)	@ e = 0.5%	@ e = 2.0%	(%)
			Solution heat treated at 768K						
68	26	463	63.4	(437)	76.3	(526)	4.9	1.43	4.2
			Solution heat treated at 788K						
171[4][6]	- as SHT -		32.8	(226)	57.5	(396)	4.34	3.17	7.0
174[5]	0.2	463	50.0	(345)	68.8	(474)	4.37	2.71	5.3
123[6]	0.75	463	60.3	(416)	76.7	(529)	5.74	0.87	3.7
124	1.75	463	63.9	(440)	78.0	(538)	5.49	0.92	3.2
121	5.0	463	66.1	(456)	79.6	(549)	5.67	0.88	3.0
122	14.0	463	71.8	(495)	81.8	(564)	4.10	0.63	3.2
67	26	463	69.9	(482)	81.1	(559)	3.66	1.37	5.1
172	30	463	67.1	(463)	77.4	(533)	4.12	1.51	3.1
173	70	463	57.3	(395)	70.4	(486)	5.55	1.39	3.9
			Solution heat treated at 808K						
66	26	463	68.6	(473)	82.9	(571)	5.86	1.68	2.8
			Solution heat treated at 828K						
167[4][6]	- as SHT -		48.8	(336)	71.3	(491)	1.99	2.56	6.5
170[5]	0.2	463	64.2	(443)	80.0	(551)	4.21	1.69	4.5
119[6]	0.75	463	67.3	(464)	81.0	(559)	4.84	1.02	3.2
120	1.75	463	65.6	(452)	82.5	(569)	5.53	1.12	3.4
117	5.0	463	69.7	(481)	86.0	(593)	5.27	0.97	3.7
118	14.0	463	71.1	(490)	85.1	(587)	5.97	0.82	3.2
65	26.0	463	76.3	(526)	84.5	(583)	3.90	0.71	2.4
70	26.0	463	76.7	(529)	88.0	(607)	4.42	1.48	3.7
168[7]	30.0	463	76.9	(531)	- -	- -	4.55	- -	- -
169	70.0	463	68.0	(469)	81.0	(559)	5.20	1.69	3.5

Table A12 (continued)

Notes: (1) Tensile round specimens nominally 32mm gage length with a 6.25mm diameter section.

(2) Tests performed in accordance with ASTM-E8 in ambient air and at an initial engineering strain rate of $1.4 \times 10^{-4}\ s^{-1}$.

(3) Specimens 65, 66, 67 and 68 solution heat treated for 0.67 hours. All others held 1 hour prior to cold water quench.

(4) Flow stress is notably strain independent at low plastic strains; (up to 0.4% strain); analogous to yield point phenomenon.

(5) Load/displacement curve strongly serrated (355N peak-to-peak); more pronounced with increasing strain.

(6) Load/displacement curve is mildly serrated (90N peak-to-peak); more pronounced with increasing strain.

(7) Threads stripped prior to specimen fracture.

Table A13

THE TENSILE PROPERTIES OF Al-Li-Cu AS A FUNCTION OF AGING CONDITIONS FOR LONG TRANSVERSE ORIENTED TENSILE ROUNDS FABRICATED FROM THE AS-EXTRUDED PLATE(1) - (4)

Specimen Designation	Aging Condition		0.2% Offset Yield Strength		Ultimate Tensile Strength		Slope of Stress/ Strain Curve (GPa)		Plastic Strain-to-fracture
	Time(hrs)	Temp(K)	Ksi	(MPa)	Ksi	(MPa)	@ e = 0.5%	@ e = 2.0%	(%)
454	7	443	54.5	(376)	65.3	(450)	2.9	1.86	3.3
455	28	443	56.3	(388)	64.5	(445)	3.78	(4)	2.0
456	90	443	56.1	(387)	65.7	(453)	4.18	1.42	2.9
457	28	443	57.1	(394)	66.9	(461)	4.26	1.81	2.7

Notes: (1) Tensile round specimens nominally 1.27mm gage length with a 3.05mm diameter section.

(2) Tests performed in accordance with ASTM E8 in ambient air and at an initial engineering strain rate of $1.4 \times 10^{-4} s^{-1}$.

(3) Insufficient strain-to-fracture to obtain data.

Table A14

THE TENSILE PROPERTIES OF Al-Li-Cu-Mg AS A FUNCTION OF AGING CONDITIONS FOR LONG TRANSVERSE ORIENTED TENSILE ROUNDS FABRICATED FROM THE AS=EXTRUDED PLATE (1) - (4)

Specimen Designation	Aging Condition		0.2% Offset Yield Strength		Ultimate Tensile Strength		Slope of Stress/ Strain Curve (GPa)		Plastic Strain-to-fracture
	Time(hrs)	Temp(K)	Ksi	(MPa)	Ksi	(MPa)	@ e = 0.5%	@ e = 2.0%	(%)
458	5	463	64.6	(445)	78.8	(543)	4.6	2.13	3.6
459	26	463	66.7	(460)	72.7	(501)	6.02	(4)	0.9
461	26	463	68.3	(471)	76.8	(530)	4.80	(4)	1.6

Notes: (1) Tensile round specimens nominally 1.27mm gage length with a 3.05mm diameter section.

(2) Tests performed in accordance with ASTM-E8 in ambient air and at an initial engineering strain rate of $1.4 \times 10^{-4}\ s^{-1}$.

(3) All specimens solution heat treated for 1 hr at 828K, then cold water quenched.strain.

(4) Insufficient strain-to-fracture to obtain data.

Table A15

The Fracture Toughness of Al-Li-Cu as a Function of Solution Heat Treatment and Aging Conditions for Compact Tension Specimens Fabricated from the As-Extruded Plate: T-L Orientation

Specimen Designation	Aging Condition		0.2% Offset Yield Strength	K_{IC}	K_Q	Invalid According to the ASTM Method E399 Section Indicated
	Time(hrs)	Temp(K)	MPa	$MPa\text{-}m^{1/2}$	$MPa\text{-}m^{1/2}$	
			Solution Heat Treat for 1 hour at 788K			
200	200	443	400	8.5	--	
210	300	443	385	--	8.3	7.42, 8.23
212	5	463	390		11.5	7.11
			Solution Heat Treated for 1 hour at 828 K			
204	200	443	426	--	8.8	7.2.1., 7.4.2
205	300	443	384	--	8.9	7.4.2
207	5	463	445	--	12.9	7.1.1

Notes: (1) Testing performed on 12.7mm thick and 25.4mm wide compact tension specimens

(2) Testing was in accordance with ASTM E399-74 excepting instances of non-compliance with requirements for valid K_{IC} determination as indicated.

Table A16

The Fracture Toughness of Al-Li-Cu-Mg as a Function of Solution Heat Treatment and Aging Conditions for Compact Tension Specimens Fabricated from the As-Extruded Plate: T-L Orientation

Specimen Designation	Aging Condition		0.2% Offset Yield Strength	K_{IC}	K_Q	Invalid According to the ASTM Method E399 Section Indicated
	Time(hrs)	Temp(K)	MPa	$\frac{}{MPa\text{-}m^{1/2}}$	$\frac{}{MPa\text{-}m^{1/2}}$	
			Solution Heat Treat for 1 hour at 788K			
218	0.4	463	375	--	15.8	7.1.1
221	14	463	495	9.6	--	
219	70	463	395	--	7.4	7.2.1, 7.4.2
			Solution Heat Treated for 1 hour at 828 K			
214	0.4	463	450	--	14.0	7.1.1, 7.2.1, 7.4.2
217	14	463	490	10.2	--	
215	70	463	469	7.5	--	

Notes: (1) Testing performed on 12.7mm thick, and 25.4mm wide compact tension specimens

(2) Testing was in accordance with ASTM E399-74 excepting instances of non-compliance with requirement (s)for valid K_{IC} determination as indicated.

SECTION B

PRELIMINARY DATA - THE STRESS CORROSION CRACKING SENSITIVITY OF Al-Li-Cu ALLOYS

LIST OF ILLUSTRATIONS

LIST OF TABLES

INTRODUCTION

The main objective(s) of the NASA-Ames Research program are to: 1) identify a practical stress corrosion cracking (SCC) screening technique, and 2) to evaluate the relative SCC resistance of Al-Li-Cu candidate advanced aluminum alloys. This work is essential for successful near-term inplementation of improved alloys for aerospace application and for the eventual development of optimum structural alloys. The purpose of Section B is to report the results of stress corrosion tests completed during the last contract period. A variety of methods for determining the resistance to stress corrosion cracking are being employed in the study. Electrochemical polarization experiments have been completed and these results are discussed. In addition, crack initiation and crack growth behavior are being evaluated for aqueous sodium chloride exposure. Preliminary data are reported.

EXPERIMENTAL TECHNIQUE

A variety of methods for determining the resistance to stress corrosion cracking (SCC) are being employed in this study. Smooth section specimens are being exposed under alternate immersion, aqueous sodium choloride conditions to determine the so-called threshold stress for SCC. The threshold stress is defined as the upper limit stress below which specimens do not fracture in a specified exposure period. Fracture mechanics (flawed) specimens are being used to evaluate the threshold stress intensity for SCC, K_{ISCC}, and to establish the relationship between the crack growth rate versus stress intensity for various electrochemical conditions. The threshold stress intensity, K_{ISCC}, is defined as that value below which a limiting value of crack growth rate is not observed in a specified exposure period. Double cantilever beam (DCB) type specimens* are being used to assess K_{ISCC}. Pre-cracked compact tension and 4-point bend specimens are being used to determine the SCC growth rate behavior. Slow strain rate tests are being performed under controlled electrochemical conditions to establish the active electrochemical regime for stress corrosion cracking. Potentiodynamic polarization measurements form the basis for the potentiostatic controlled slow strain rate tests.

The tuning fork crack initiation specimen selected to this program is illustrated in Figure B1. The specimen geometry was suggested in ASTM STP 425, Stress Corrosion Testing, Proceedings on the Atlantic City Symposium on Stress Corrosion Testing, 1966. A surface area of about 5 cm^2 is maintained at constant

---

* Mostovoy, Sheldon, Crosley, P.P., and Ripling, E.J., Use of Crack-Line-Loaded Specimens for Measuring Plane-Stress Fracture Toughness", Journal of Materials, Vol 2,No.3,Sept. 1967, pp. 661-681.

stress using this specimen configuration. Tuning fork specimens were fabricated from the as-extruded plate. Specimens were oriented so as to promote crack initiation along a plane where normal is the transverse (T) direction, and crack growth in the short-transverse (S) direction. After fabrication, specimens were solution heat treated, quenched and aged to the desired condition. The base alloy (Al-Li-Cu) specimens were aged at 170°C for 26 hours; the magnesium base alloy specimens were aged 26 hours at 190°C. The respective mechanical properties are reported in Section A.

The gage surfaces of tuning fork specimens were rough polished to 600 grit finish prior to exposure. Constant deflection specimens were strain gaged to monitor crack initiation events through load drop at constant deflection. The constant deflection conditions were maintained via single bolt loading. Stainless steel bolt and nut combinations were used, and strain gage out-put was used to determine the initial loading stress. Other tuning fork specimens were dead weight loaded in a stress corrosion facility designed for the alternate immersion tests. The initial stress upon loading was calculated from the elastic equation for cantilever beam loading. Tuning fork specimens were alternately immersed in the 3.5 % NaCl (pH $\sim$ 6.8) solution, then air dried. The salt solution was maintained at 30°C. The 3.5% NaCl content was monitored using a precision hydrometer and adjusted through addition of either distilled water or reagent grade NaCl, as required. The reservoir for the alternate immersion test contained approximately 35 liters; the solution was circulated to specimens for 10 minutes each hour resulting in a ten minute wet/50 minute dry immersion cycle. The NaCl solution was changed every two weeks. Specimen failure was indicated by either change in LVDT output from the load line of the constant load test, or from drop in strain gage output from the constant deflection instrumented specimens. A Sun System Data Acquisition System was used to continuously monitor test conditions.

Twelve DCB specimens were fabricated from solution heat treated and quenched plate per the requirements of Figure B2. Specimen orientation was S-L, thus promoting crack extension on a plane normal to the short transverse direction in the longitudinal (or extrusion) direction Specimens were aged after fabrication. Base alloy (Al-Li-Cu) specimens previously solution heat treated at 515°C were aged 80 hour at 170°C. The Al-Li-Cu-Mg alloy specimens, solution heat treated at 555°C, were subsequently aged 30 hours at 190°C. The respective mechanical properties are tabulated in Section A of the report. After aging, specimen sides were polished to 1 μm diamond and lines were scribed at appropriate distances to monitor crack extension.

Prior to aqueous sodium chloride exposure, DCB specimens were fatigue pre-cracked under strain controlled conditions using a closed loop electrohydraulic test system. Pre-cracking was performed at $10H_Z$ and the maximum stress intensity during pre-cracking did not exceed 80% of the value targeted for start-up of the threshold stress intensity study. Pre-cracking was performed in air, and the final crack length was approximately 18 mm.

After pre-cracking stainless steel bolts were used to load DCB's. Specimens were soaked in 3.5% NaCl solution ten minutes prior to bolt loading. A clip-on extensometer was used to monitor the load line displacement. Six of each alloy type were thus loaded to stress intensities ranging from 6 to 8 MPa-$m^{1/2}$. An upper limit of 8 MPa-$m^{1/2}$ was selected as this is the approximate K_{IC} value for these Al-Li-Cu alloys (see Section A). After loading, specimens were immersed in 3.5% NaCl solution, and twice a week crack extension or monitored. Tests are on-going. Each week the solution has been changed in the approximate one liter immersion reservoir. Conditions are static, and the temperature of the solution is maintained at 30°C.

In preparation for the slow strain rate tests, anodic potentiodynamic polarization measurements were made on duplicate specimens. Cylindrical specimens were machined from extruded plate previously heat treated at 555°C and cold water quenched. After fabrication, specimens were aged, then polished on a bench lathe to a 1 μm diamond finish. Specimens were degreased then rinsed in freon prior to salt water immersion. Upon attachment to the working electrode of the polarization cell, specimens were immersed in a stirred helium and deaerated 3.5% NaCl solution and after a maximum of 40 minutes, the potential was driven from a value more anodic than the rest potential to a value more cathodic than the breakaway potential. A Wienken potentiostat and motor driven scan generator were used to vary the electrochemical potential. The solution was deaerated by bubbling He for 24 hours prior to and during each scan. The potential scan rate was 10 mv/min and the current vs. potential curve was recorded on an X-Y recorder. Measurements were made in accordance with ASTM G5 excepting minor variations to assume reproducibility of results, such as an extended deaeration and pre-soak cycle.

The anodic polarization curves were found to be very sensitive to (1) the surface condition of the sample, (2) the soaking period prior to start of the potential scan and (3) the "condition" of the polarization cell solution. For example, a milky white corrosion residue collected during each potentiodynamic scan, and the accumulation of the substance appeared to influence subsequent polarization data. Because of this, the solution in the polarization cell required frequent changing. Care was also required to assure that fresh solution was adequately deaerated. Dearation was assisted by heating the solution to about 45°C for the first few hours, then cooling to the test temperature of 30°C. Inert gasses such as N_2 and Ar proved much less efficient than He in deaerating the polarization cell solution.

RESULTS AND DISCUSSION

Polarization Data

Polarization data for the base alloy as a function of aging condition are presented in Figures B3-B5. Polarization data for the magnesium bearing alloy are presented in Figures B6-B8. The electrochemical potential is referenced to the standard calomel electrode (sce); positive potentials are cathodic and negative potentials anodic. Potentiodynamic curves for the Al-Li-Cu alloys exhibited passive/transpassive behavior. Five electrochemical parameters were selected to characterize the polarization behavior. They are as follows:

1) The rest potential - the potential of the working electrode with respect to the reference electrode after initial immersion and under open circuit potentiostatic conditions.

2) The zero current potential - the potential at zero current as the working electrode potential is swept from a value more anodic than the rest potential to a value more cathodic. The rest potential and the zero current potential should essentially be equivalent.

3) Current spike potential - the potential during sweep toward increasingly greater cathodic potentials and prior to the breakaway potential, where current spikes begin to occur. This signifies instability of the passive layer.

4) Passive current density - the current density (in μA per cm^{-2}) in the passive regime where the cell current is independent of potential.

5) The breakaway potential - the potential during sweep to more cathodic potentials where the anodic polarization current exponentially increases. It marks transition from passive to transpassive behavior.

Review of the polarization data of figures B3 thru B8 indicate the following. On the basis of the more anodic rest and/or zero current potential and the higher passive current density, the magnesium bearing alloy (solution heat treated at 555°C), is predicted to exhibit the greatest tendency for corrosion. Indeed, both Al-Li-Cu alloys demonstrate increasing corrosion tendency for the higher solution heat treatment temperature. However, aging condition appears to have little systematic influence on the electrochemical parameters. The most consistent trend is a slight decrease in the breakaway potential (increasingly more anodic) with aging time noted for both Al-Li-Cu alloys.

It was hoped that the polarization data would provide a means of identifying aging conditions that would be sensitive to the stress corrosion cracking phenomenon. However, this technique appears to be relatively insensitive to microstructural variations which occur for the under, peak, and overaged conditions of interest in the Al-Li-Cu alloy system. In addition, difficulty is anticipated in being able to maintain constant electrochemical conditions because of specimen surface, deaeration, and water chemistry variation which will occur during prolonged periods of potentiostatic control. Thus difficulty is anticipated for the slow strain rate experiments soon to be initiated. Yet the usefulness of the polarization data can not be properly assessed until the data are correlated with stress corrosion test results. Slow strain rate tests will be run at various strain rates and at various potentials within the passive regime to evaluate possible correlation to the data of Figures B3-B8.

Alternate Immersion Crack Initiation and Growth Data

The first alternate immersion tests (per ASTM Method G44-75) for evaluating the combination of crack initiation and crack growth (initial stress vs. time to failure) have been completed. The tests duration was up to 84 days and the data are summarized in Figure B9. As can be seen, failures were observed in both of the Al-Li-Cu alloys. The 7075-T6 alloy loaded to the highest stress level investigated did not fail or show any evidence of cracking. The dashed curve on Figure B9 is the approximate lower bound for stress corrosion of 7075-T6 having a similar grain aspect ratio as the Al-Li-Cu alloys. As is seen, both Al-Li-Cu alloys appear more susceptible to stress corrosion crack initiation than 7075 with the magnesium bearing alloy being the most susceptible. Also shown on this figure is a scanning electron micrograph of a typical stress corrosion crack observed in the Mg bearing alloy. If these alternate immersion tests results are normalized in terms of fracture toughness, which defines the flaw size prior to catastrophic crack extension, the relative SCC sensitivities of 7075-T6 vs the Al-Li-Cu alloys would require adjustment. This will be considered in the final interpretation of the alternate immersion tests currently in progress.

The Al-Li-Cu alloys which did not fail after the 84 day alternate immersion test were mildly pitted and did contain stress corrosion cracks about 0.25mm deep. The surviving 7075-T6 aluminum specimens were severely pitted but crack initiation had not occured. Because the 3.5 sodium choloride solution (pH = 6.8) promoted generalized pitting of test specimens, subsequent tests are being performed in substitute ocean water (without heavy metal additions) prepared in accordance with ASTM Specification D 1141.

Stress Corrosion Crack Growth Rate Data

Six base alloy and six magnesium bearing alloy DCB type specimens in the peak aged condition were precracked and bolt loaded to an initial stress intensity of from 6 to 8 MPa-$m^{1/2}$. Specimens are S-L oriented so as to assess K_{ISCC} in the most stress corrosion susceptible microstructural condition. The DCB specimens were immersed in sodium chloride solution during bolt loading, and subsequently immersed and maintained in 3.5% NaCl at 30°C. To the present (an accumulated exposure period of 120 days) only limited crack extension has occured even though the applied stress intensities are very close to K_{IC}. One thought is that general corrosion in the aqueous chloride environment is blunting the crack tip. Similar tests are planned for a less severe environment of water sequencing to HCL additions and/or substitute ocean water where sustained "macro" crack growth will first be substantiated in constant displacement tests conducted in closed loop electrohydraulic mechanical test frames.

The critical stress intensity for stress corrosion cracking, K_{ISCC}, in salt water is greater than 8 MPa-$m^{1/2}$ for some commercial 2XXX series alloys. Thus, this may be true for the Al-Li-Cu alloys. Since the K_{IC} value for the S-L oriented DCB's is about 8 MPa-$m^{1/2}$, the ability to determine K_{ISCC} is limited. To improve this situation, compact tension specimens L-T oriented are being fabricated. The fracture toughness in the L-T orientation is anticipated to be greater than either, the T-L or S-L orientations. Compact tension specimens tested under crack opening displacement control will then be used to further assess crack extension of the Al-Li-Cu alloys in a substitute ocean water environment.

During the alternate immersion tests and DCB exposure of Al-Li-Cu specimens, a milky white corrosion residue accumulated.

In order to investigate the nature of the corrosion in 3.5% aqueous NaCl solution, samples of the residue and of the reservoir solution where analyzed. The respective analyses are indicated in Table B1. Comparison of the solution before and after two weeks of corrosion of tuning fork specimens of both Al-Li-Cu alloy types indicates an increase in the aluminum, copper and nickel contents.

The milky white corrosion residue collected from the immersion solution of the DCB specimens is high in aluminum, copper, silicon, iron, zinc, lead, tin and boron. Manganese, titanium and chrome were found in lesser amounts. As foreign substances were not intentionally introduced, it would appear that (1) the stainless steel loading bolts are not totally protected by the paraffin coating employed, or (2) that the Pyrex glass is not immune to attack or dissolution in the salt solution. Note that lithium above the detection limit was not found in either the corrosion residue or salt solution: it would appear that the lithium forms an insoluble corrosion product.

SUMMARY

A variety of methods for determining the resistance to stress corrosion cracking (SCC) are being employed in this study. Smooth section tuning fork specimens exposed under 3-1/2% salt water alternate immersion conditions, are being used to determine the so-called threshold stress for SCC. Fracture mechanics specimens are being used to evaluate K_{ISCC} and to establish the crack growth rate behavior under various electrochemical conditions. Slow strain rate tests are being performed under potentiostatic control to establish the active electrochemical region for SCC and to further analyze crack initiation in the Al-Li-Cu alloys. The objective of the initial research is primarily to identify a practical stress corrosion screening technique for advanced aluminum alloy for aerospace application.

In preparation for the slow strain rate tests, polarization data were obtained for a broad range of aging conditions. The higher passive current density and the lower (more anodic) rest potential of the magnesium bearing alloy indicate a greater tendency for general corrosion to occur with respect to the base alloy. Aging these alloys, however, is found to have little systematic influence on the electrochemical parameters. That is, the potentiodynamic technique is relatively insensitive to microstructural variations which occur as a result of aging. In addition, difficulty is anticipated in being able to maintain constant electrochemical conditions due to variations in the surface condition (sample-to-sample), degree of deaeration, and water chemistry during prolonged periods of potentiostatic control. This is cause for concern in the performance of the slow strain rate tests. However, the formation of an unstable, passive film in sufficiently deareated salt solution was confirmed in the electrochemical tests. Competition of the formation of this film with newly exposed metal surface during the slow strain tests may define regimes of stress corrosion susceptibility.

Efforts to define K_{ISCC} using pre-cracked and bolt loaded DCB specimens were hampered by aggressive general corrosion in the 3-1/2% NaCl solution and by the inherent low fracture toughness of the reference alloys. Limited crack extension was observed in specimens loaded close to K_{IC} after 120 day exposure. Subsequent tests will be performed in less aggressive substitute ocean water per ASTM specification D1141.

The first alternate immersion tests per ASTM Method G44-75 have been completed. Both Al-Li-Cu alloys appear more susceptible to stress corrosion crack initiation than 7075-T6 aluminum with the magnesium bearing alloy being the most susceptible. Initial tests were performed in 3.5% sodium chloride solution; and local pitting was observed for both Al-Li-Cu alloys. Current tests are being performed in substitute ocean water per ASTM Specification D1141.

Conclusions

1. On the basis of a more anodic rest potential and higher passive current density, the magnesium bearing alloy is predicted to exhibit the greater tendency for corrosion when compared to the base Al-Li-Cu alloy.

2. The potentiodynamic technique appears to be relatively insensitive to microstructural variations which occur for the under, peak and overaged conditions of interest in the Al-Li-Cu alloy system.

3. It is difficult to establish reproducible electrochemical conditions for Al-Li-Cu in deaerated 3.5% NaCl solution because of variations in the surface condition (sample-to-sample), the degree of deaeration and the local water chemistry. This is cause for concern in the performance of the slow strain rate tests.

4. General corrosion and localized pitting observed for both alloys in an aqueous 3.5% NaCl solution tend to obscure the K_{ISCC} and crack initiation experimental results. Subsequent testing shall be performed in the less aggressive substitute ocean water solution recommended in ASTM Specification D1141.

5. The inherent low fracture toughness (8 MPa-$M^{1/2}$) of the Al-Li-Cu alloys combined with crack blunting resulting from the agressive attack of the 3.5% NaCl are hampering efforts to determine K_{ISCC} using fracture mechanics type specimens. Limited crack extension has occurred for DCB specimens bolt loaded to within 10% of K_{IC} after 120 day exposure.

FIG. B1: TUNING FORK TYPE CRACK INITIATION SPECIMEN

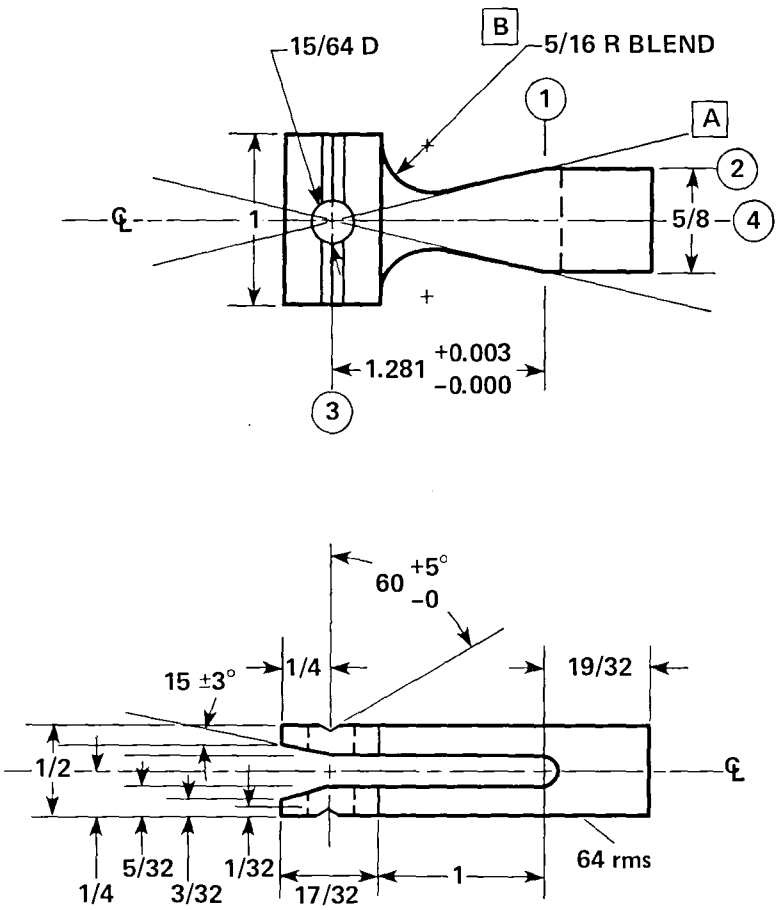

DIMENSIONS
IN inches

A. SET TAPER THRU CENTER OF 15/64 D HOLE, INTERSECTION OF (3) - (4), AND THRU INTERSECTION (1) - (2); SYMMETRIC.

B. 5/16 R TANGENT TO 17/32 in. TAB WIDTH AND TO TAPER LINE.

C. SURFACES SHALL BE PERPENDICULAR AND PARALLEL, AS APPLICABLE TO WITHIN 0.001 in. TIR.

D. RADIUS AT BOTTOM OF GROOVE SHALL BE 0.010 TO 0.020 in.

FIG. B2: DOUBLE CANTILEVER BEAM (DCB)
TEST SPECIMEN

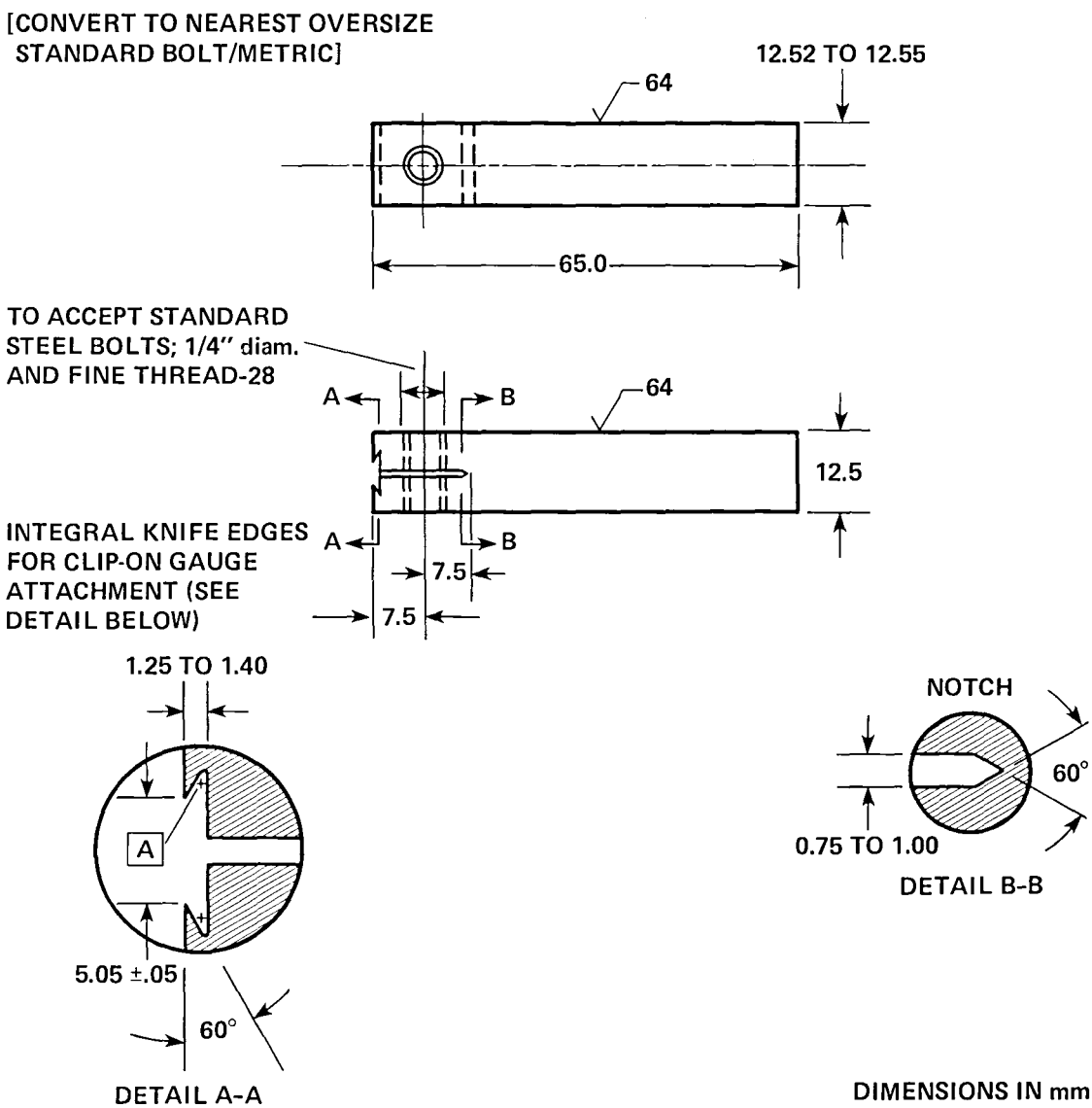

NOTES:

A. INCLUDE RADIUS ($r \cong 0.3$ mm) AT BASE OF 60° ANGLE (2 PLACES).

B. ALL DIMENSIONS IN mm EXCEPTING CALLOUT FOR 1/4"-28 DRILL AND TAP, THROUGH BOLT HOLE.

C. SURFACES SHALL BE PERPENDICULAR AND PARALLEL AS APPLICABLE TO WITHIN 0.025 mm TIR.

D. ALL DIMENSIONS ±0.05 mm UNLESS OTHERWISE INDICATED.

FIG. B3: POLARIZATION DATA AS A FUNCTION OF AGING CONDITIONS FOR Al-Li-Cu SOLUTION HEAT TREATED AT 555°C FOR 1 HOUR

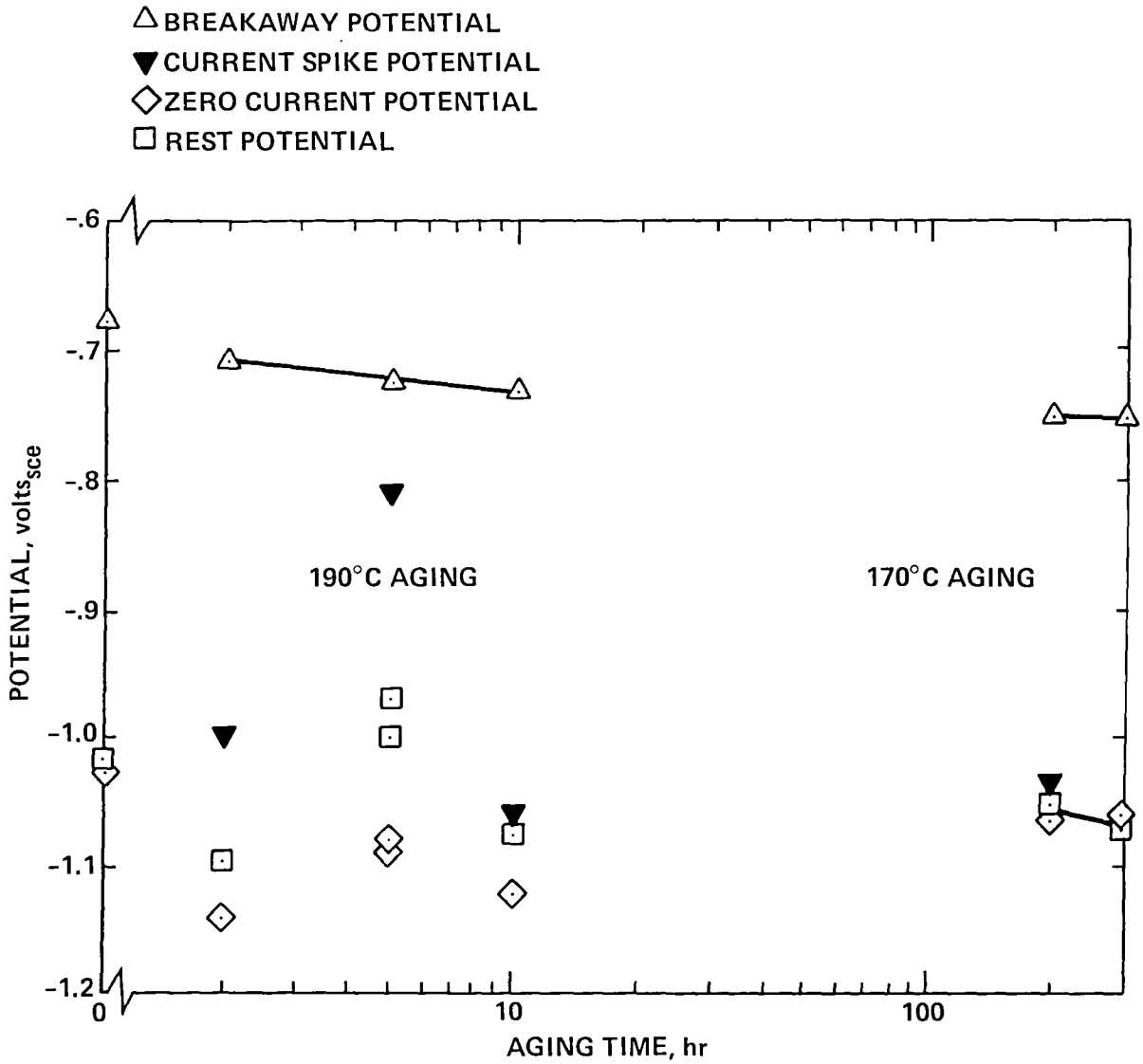

FIG. B4: POLARIZATION DATA AS A FUNCTION OF AGING CONDITIONS FOR Al-Li-Cu, SOLUTION HEAT TREATED AT 515°C/1 hr

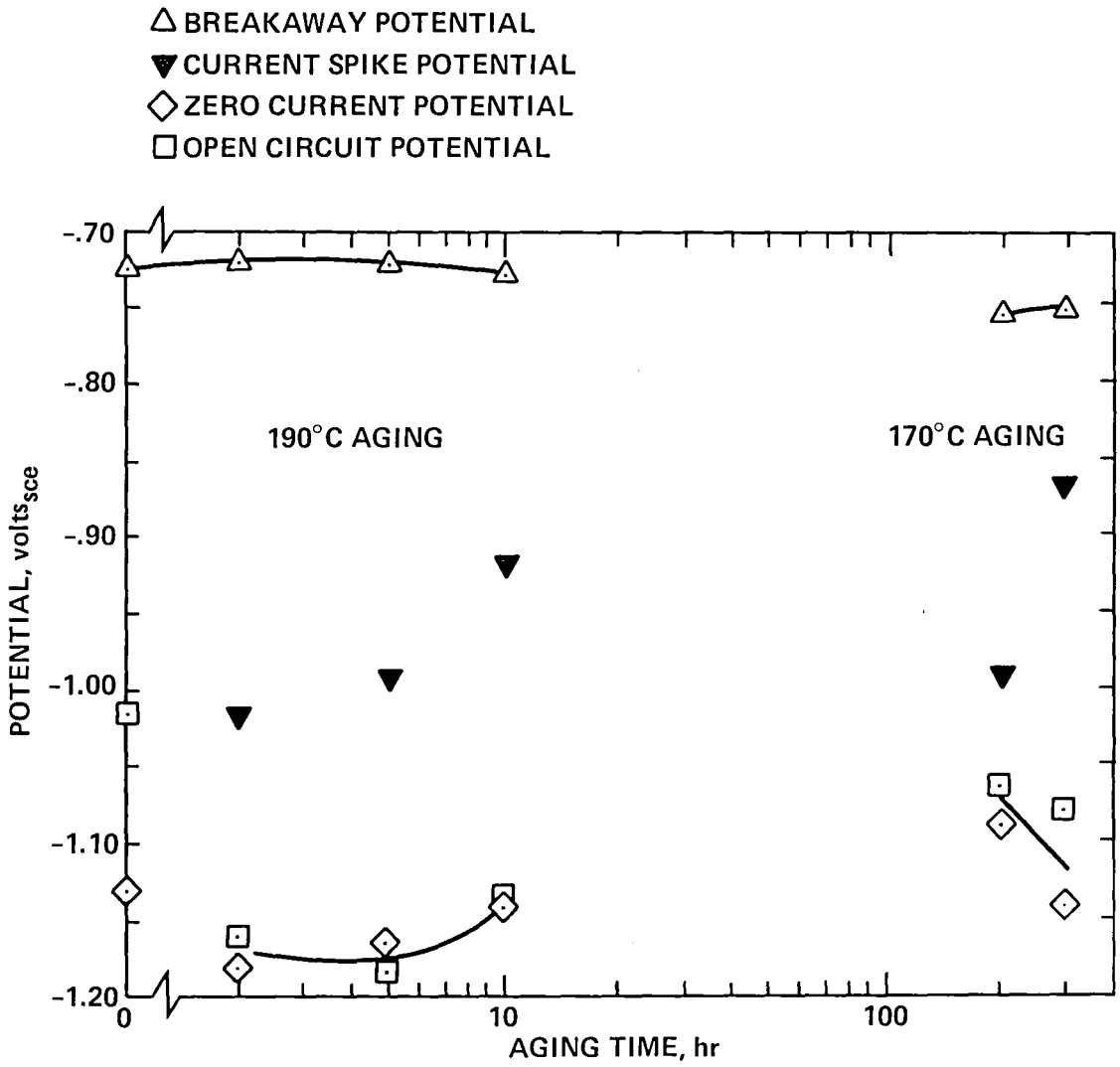

FIG. B5: THE PASSIVE CURRENT DENSITY AS A FUNCTION OF AGING CONDITIONS: Al-Li-Cu

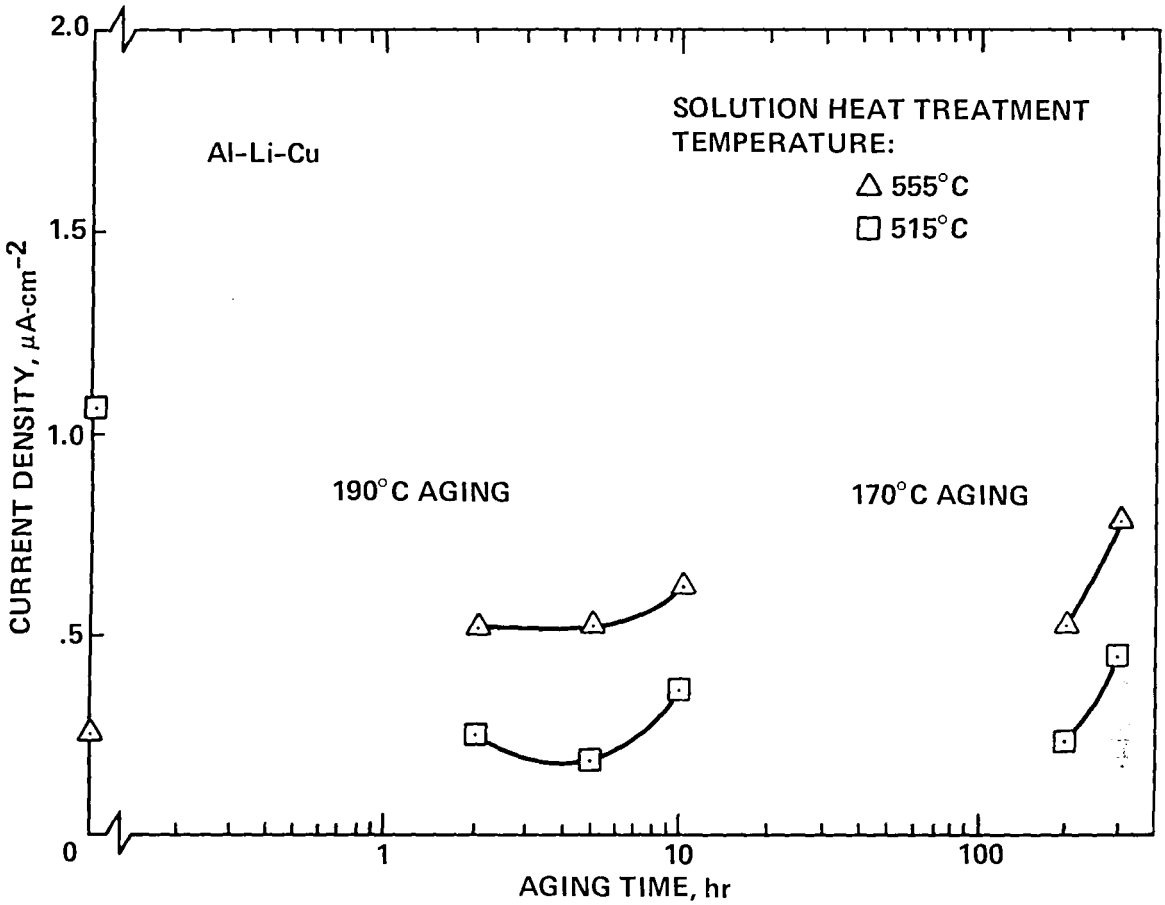

FIG. B6: POLARIZATION DATA AS A FUNCTION OF AGING THE TIME FOR Al-Li-Cu-Mg, SOLUTION HEAT TREATED AT 550°C FOR 1 HOUR

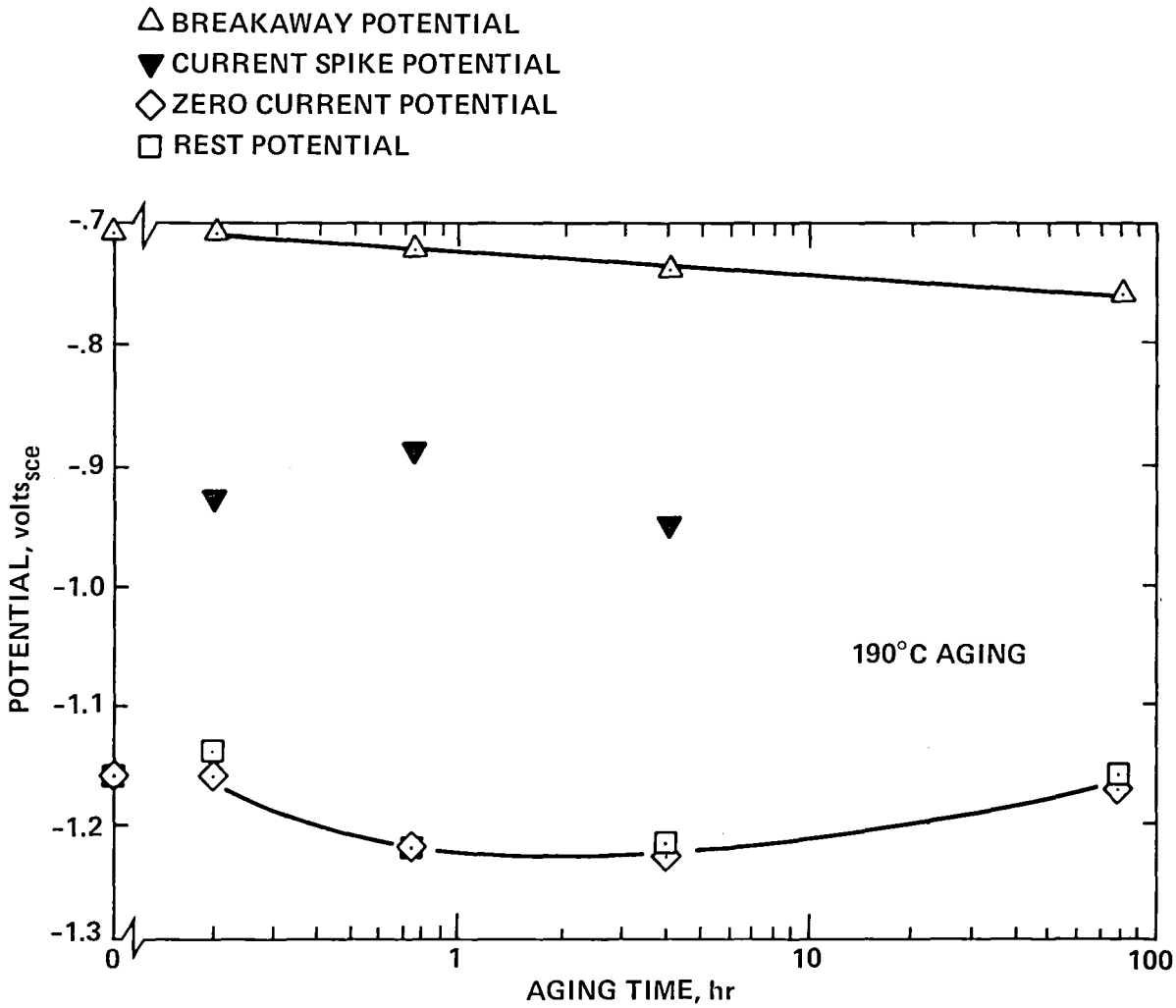

FIG. B7: POLARIZATION DATA AS A FUNCTION OF AGING TIME FOR Al-Li-Cu-Mg SOLUTION HEAT TREATED AT 515°C FOR 1 HOUR

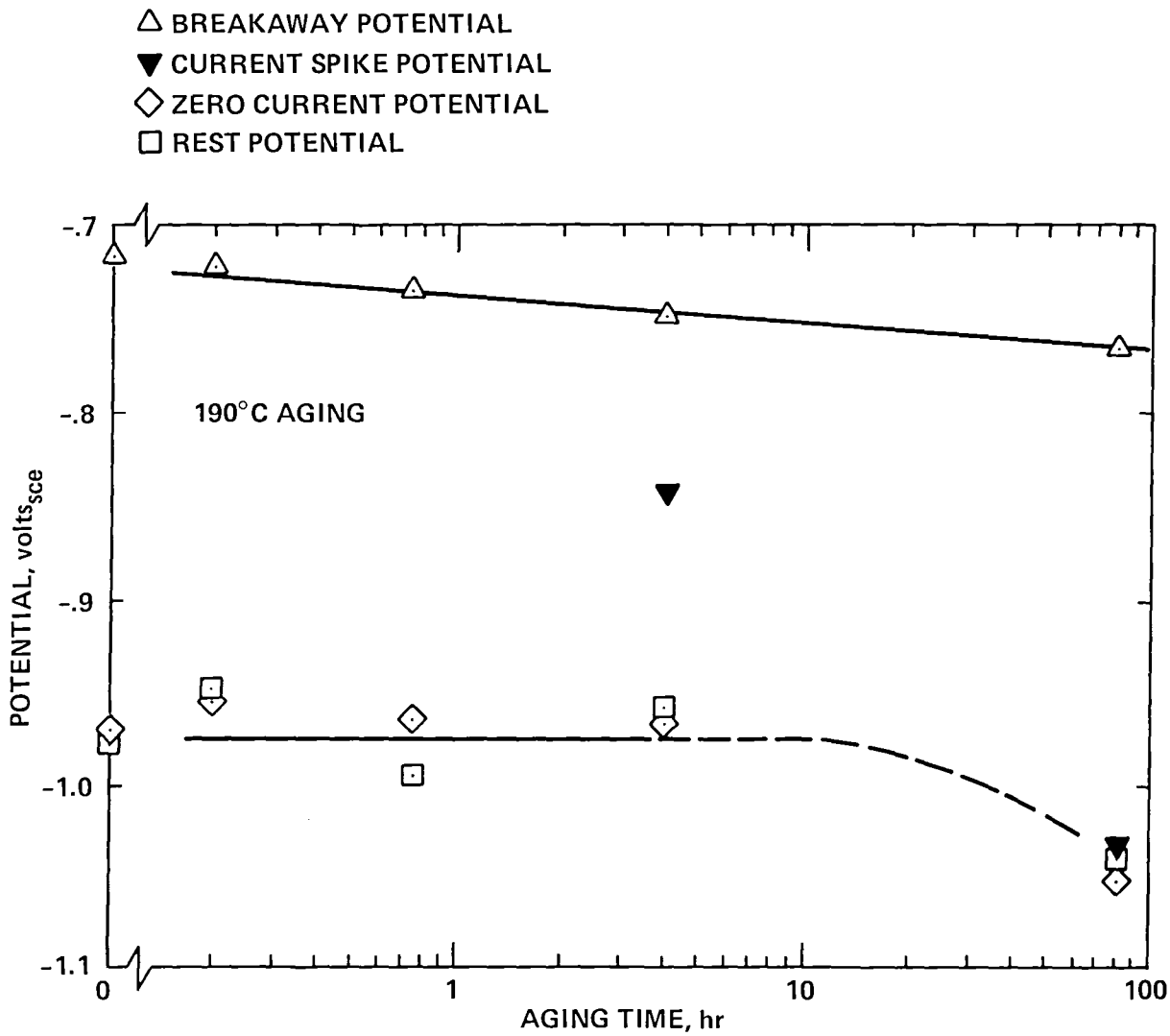

FIG B8: THE PASSIVE CURRENT DENSITY AS A FUNCTION OF AGING TIME: Al-Li-Cu-Mg

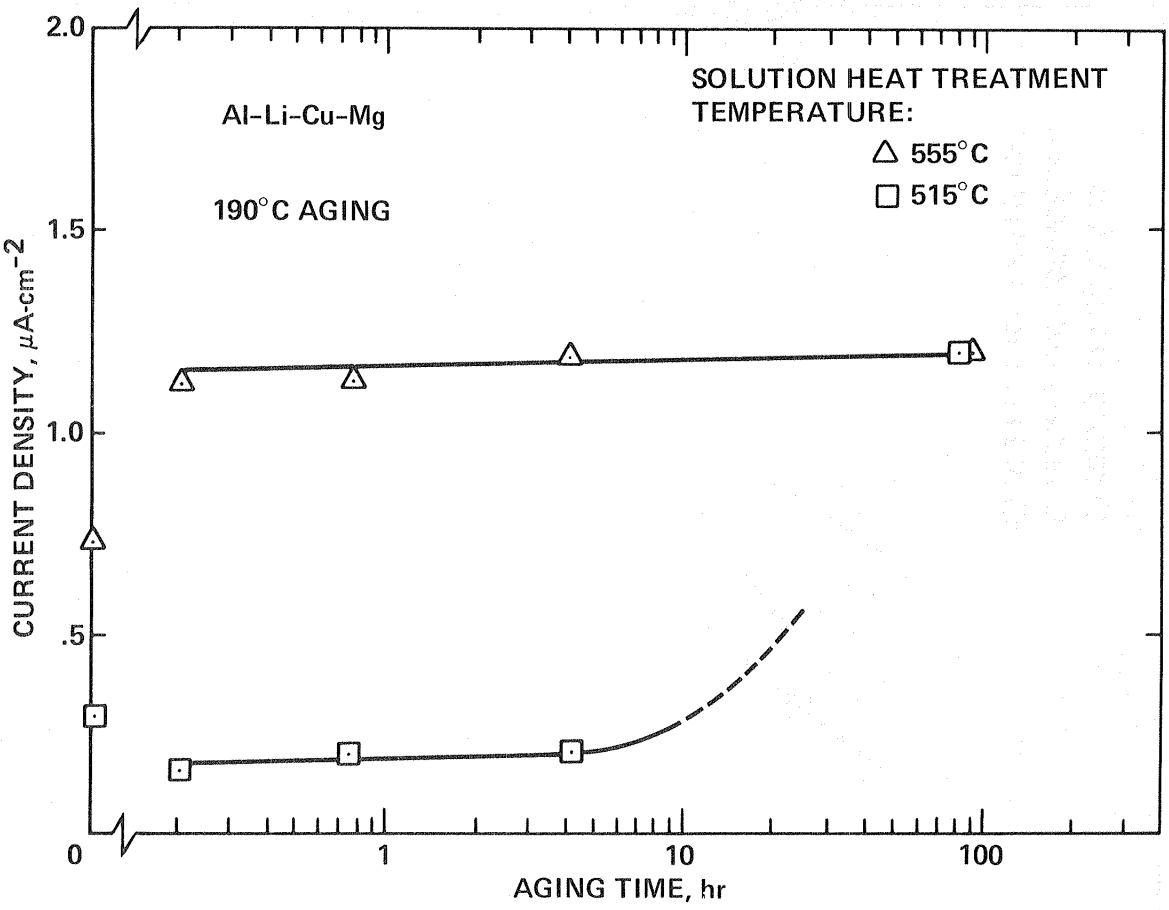

FIG. B9: AQUEOUS CHLORIDE STRESS CORROSION OF TWO Al-Li-Cu P/M ALLOYS

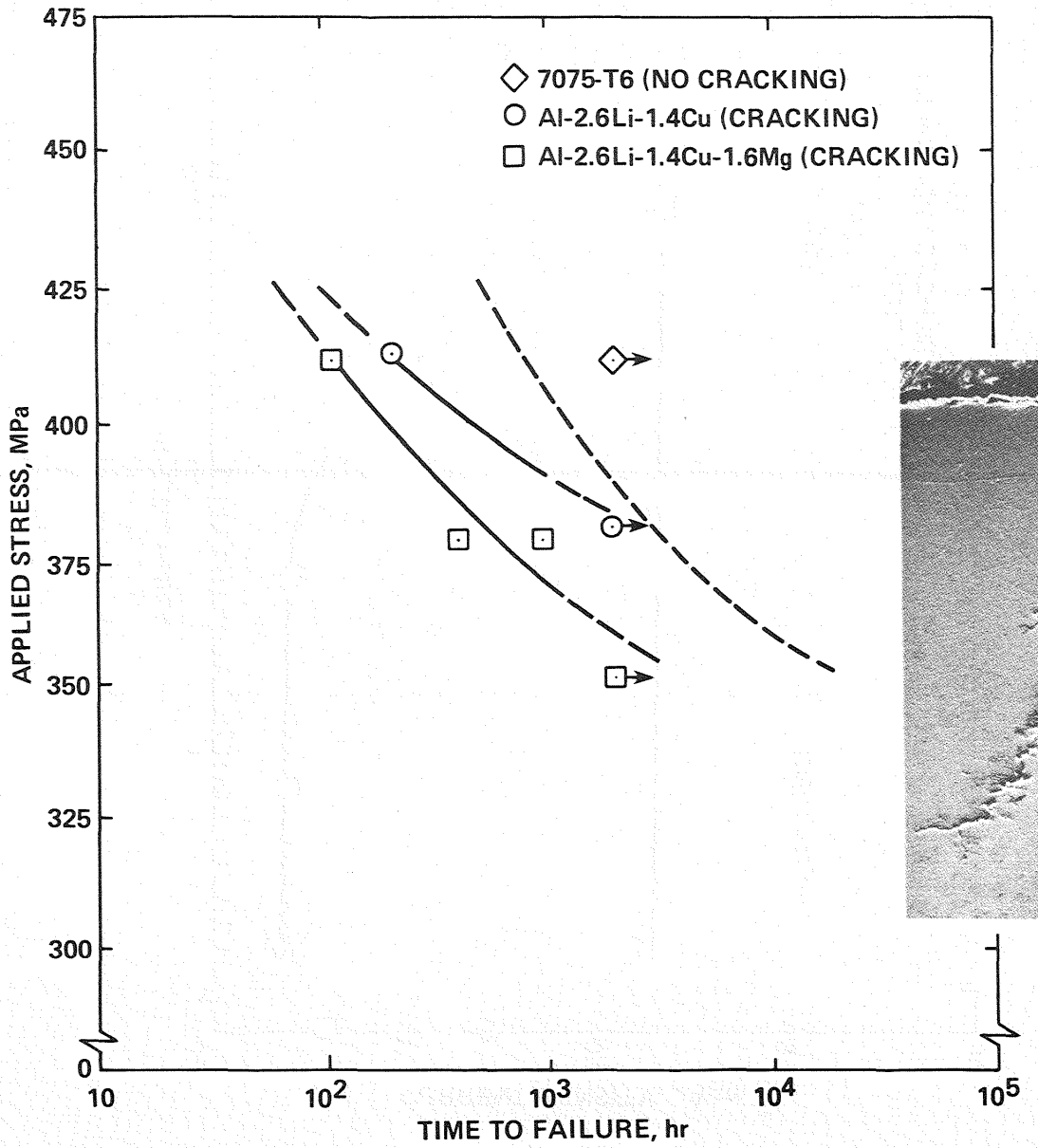

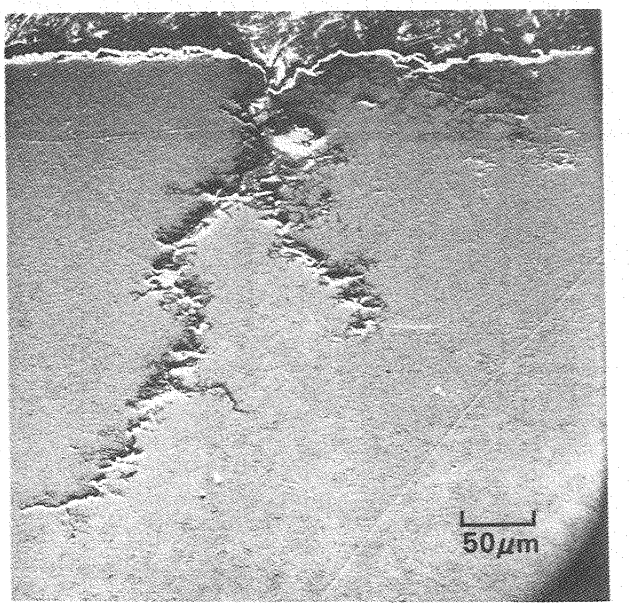

STRESS CORROSION CRACK IN THE Al-Li-Cu-Mg ALLOY

Table B1

Chemical Analysis of Aqueous Na/Cl Test Solution and Soluble Corrosion Residue

Element	Aqueous NaCl Solution Prior To Al-Li Alloy Corrosion (1)	Aqueous NaCl Solution After Two Week Exposure in SCC Facility (1)	Soluble Corrosion Residue Collected in SCC Facility (2)
	ppm by wt	ppm by wt	by weight
Al	0.1	0.3	Remainder
Li	0.7	0.5	(3)
Cu	0.5	2.0	4.78%
Mg	0.2	0.1	3ppm
Zr	0.1	0.1	=
Si	-	-	8.55%
Fe	20.0	10.0	0.24%
Mn	-	-	50ppm
Zr	0.5	0.5	0.79%
Ti	-	-	80ppm
Ni	0.3	0.7	-
Cr	-	-	8ppm
S	-	-	0.025%
Pb	-	-	0.055%
B	-	-	0.065%
NaCl	3.5% NaCl measured by precision hydrometer: routinely monitored		

Notes: (1) Approximate 0.5 liter sample taken from continuously stirred 30 liter reservoir of SCC facility

(2) Corrosion residue accumulate from multiple 2-week exposures of 11 DCB specimens immersed in 3.5% NaCl Solution in a 2 liter pyrex glass container. Both base alloy and magnesium bearing alloys present.

(3) Element concentration below detection limit

SECTION C

THE AGING RESPONSE OF TWO ALUMINUM-LITHIUM-COPPER POWDER METALLURGY ALLOYS: A COMPARATIVE STUDY

BACKGROUND

The first annual report presented mechanical properties data acquisitioned through September 1980. These data demonstrate the tensile properties of the two reference Al-Li-Cu alloys to be a complex function of processing and heat treatment variations. Need for further characterization was expressed, particularly to demonstrate satisfactory reproducibility of properties for specimens to be used in the stress corrosion program. During the current contract period, the required testing has been completed, and the results are reported in Section A of this report. In Section C a comprehensive overview comparing the base alloy to the magnesium bearing alloy is presented. The objective will be to demonstrate key differences in the age hardening and fracture characteristics of the two alloys. Microstructural instability in response to process variations will also be compared. This overview was presented at the Fall Meeting of TMS-AIME in Louisville, Kentucky (October 1981). The viewgraphs of that presentation have been included to document the comparison.

OVERVIEW

A lot of attention has recently been focused on aluminum-lithium alloys for advanced aerospace application. These alloys may offer a strength-to-weight and stiffness-to-weight advantage of from 20 to 30 per cent over existing commercial aluminum alloys. Attention at NASA-Ames Research Center has been concerned with the environmental sensitivity of these alloys. Under Contract NAS-10365, research at the Center is addressing the stress corrosion properties of two reference Al-Li-Cu powder metallurgy (P/M) alloys. The purpose of this dicussion is to document and compare the mechanical properties and fracture characteristics of these alloys. An overview of the presentation is provided in Viewgraph (VG) C2. First the

LIST OF VIEWGRAPHS

chemical composition of the two Al-Li-Cu alloys and the powder metallurgy processing steps used to produce the alloys are reported. Next, the alloys are compared in terms of age hardening, strengthening, and ductility characteristics. The fracture characteristics are then compared. And lastly, a difference in microstructural stability in response to hot rolling will be demonstrated.

Alloy Description

The nominal composition of the alloys of this study are presented in VG C3. The base alloy contains 2.6% lithium and 1.4% copper. The magnesium bearing alloy has the same lithium and copper contents, but also contains 1.6% Mg. Both alloys contain about 0.1% zirconium for microstructural stability.

Both alloys were powder metallurgy processed and the P/M processing steps are indicated in VG C4. Powders were produced by quickly cooling an atomized molten stream of the high purity Al-Li-Cu alloys in an argon atmosphere. The cooling rate was about 103 K/s, thus not qualifying the powders as "rapidly solidified". The rapid solidified powder (RSP) approach is also being investigated in concurrent advanced Al-Li alloy development programs in the U.S. Powder particles were spherical and about 150 μm in diameter. Powders were packed in a 6061 aluminum alloy can, degassed, and cold isostatic pressed to 415 MPa. The billet was then hot upset at 480°C, and extruded at 400°C through a 2 1/2 by 2 1/2 inch round corner die. The maximum extrusion ration is about 10:1.

Age Hardening, Strengthening and Ductility Characteristics

VG C5 lists the mechanical properties characteristics to be compared in VG C6 thru VG C9. First, the age hardening response is ilustrated. Secondly, trend curves for the yield stress and ultimate tensile stress as a function of aging time

and temperature are illustrated. Finally, the ductility as monitored by the plastic strain-to-fracture of the two Al-Li-Cu alloys is compared.

In VG C6, the age hardening is plotted as a function of aging time at an aging temperature of 190°C. The superficial hardness (Rockwell 15-T) scale was used to monitor hardness. Data for both the base alloy and for the magnesium bearing alloy are presented. The solution heat treated hardness is indicated at zero aging time.

The magnesium bearing alloy achieves a higher peak hardness (88 vs 84 R/15-T); but the aging time to peak hardness is longer for Al-Li-Cu-Mg. Note, however, that at relatively short aging times ($t < 50$ minutes) the magnesium bearing alloy appears to rapidly harden. This anomalous aging behavior is also observed in the tensile strength versus aging time curves, and is the subject of the time temperature parametric analysis of Section D. The presence of magnesium will be shown to affect the kinetics of the age hardening processes within the Al-Li-Cu alloys.

The yield stress, YS, and ultimate tensile stress, UTS, of the base and magnesium bearing alloys as a function of aging at 190°C are presented in VG C7. Trend curves consistent with the age hardening curves of VG C6 result. The magnesium bearing alloy achieves a peak strength approximately 12% greater than the base alloy. The peak strengthening kinetics are more sluggish in the alloy containing 1.6% Mg, but the early precipitation strengthening kinetics are more rapid.

The ductility characteristics, as monitored by the plastic strain-to-fracture, are compared for the base and magnesium bearing alloys in VG C8. Yield stress and ductility curves for the magnesium bearing alloy aged at 190°C are presented. Analogous curves for the base alloy are present, but for an aging temperature of 170°C. Ductility data have been included in addition to the trend curve for the base alloy to illustrate

the degree of scatter. The ductility of the as solution heat treated base alloy are indicated by the open squares at zero aging time; the solid line at zero aging time denotes the e_f value for the magnesium bearing alloy in the as solution heat treated condition. The yield strength trend curves have been included to establish the relative under, peak, and over aged conditions. All data represent the as-extruded alloy. The load axis of the tensile specimens is oriented parallel to the extrusion direction.

The strain-to-fracture of the base alloy does exhibit an inverse relationship with respect to the yield strength, as anticipated. The as solution heat treated fracture strain is 8.5%. Near the peak aged condition, the fracture strain decreases to 3.0%. With overaging, the strain-to-fracture increases but much scatter is evident. Fracture strains range from less than 3% to about 5% for 200 hour aging.

The magnesium bearing alloy has an initial fracture strain of about 7% for the as solution heat treated condition. With increased aging time the fracture strain decrease to 3.5%. As the overaged condition is approached the strain-to-fracture remains constant. This may be due to extensive grain boundary precipitation in the magnesium bearing alloy. The fracture characteristics will be compared in subsequent discussion.

The tensile properties for the peak aged condition are summarized in V6 C9 for the two alloys. The base alloy has strengths, yield and ultimate tensile, of 460 MPa and 555 MPa, respectively, and a fracture strain of 3%. The magnesium base alloy has a yield strength of 520 MPa and an ultimate tensile strength of 600 MPa. The fracture strain is about 3.5%. Limited reduction-in-area was observed in both alloys. Serrated flow (or discontinuous yielding) was noted, particularly for the magnesium bearing alloy at early aging times. This serrated flow has been observed in aluminum-3% Mg alloys and

the 7000 series aluminum alloys,, and it is usually attributed to the presence of the mobile magnesium solute atoms and their interaction with moving dislocations.

Fracture Characteristics

The next series of viewgraphs, VGC11 through VGC13, compare the fracture characteristics of the base and magnesium bearing alloys. Typical fracture profile are compared in the top half of VGC11. The base alloy fractures along the plane of maximum shear stress while the magnesium bearing alloy fractures along the plane of maximum tensile stress.* The lower half of VG11 illustrates the fracture surfaces of the respective specimens. The fracture topographies of the respective surfaces are depicted in VG C12. The base alloy exhibits a relatively brittle, stepped topography while the magnesium bearing alloy fractures intergranularly.

The brittle stepped regions are thought to correspond to crystallographic slip planes along which deformation is localized in the Al-Li-Cu alloys. Slip is constrained to slip bands due to the ordered nature of the δ' precipitation. Slip continues until pile-up stresses are sufficient to cause slip plane decohesion. Both alloys are thought to have a strong preferred orientation, and thus, a relatively flat, stepped topography is expected. The shear fracture mode, typical of the base alloy over a broad range of aging conditions,is also observed for the magnesium bearing alloy in the as solution heat treated condition and for early aging times (less than 5 hr at 190°C).

---

* The base alloy has recently been noted to transition from slip fracture to transverse fracture for the overaged condition (200 hours at 170°C). The fracture mode has not to date been evaluated.

The typical fracture mode for the magnesium bearing alloy is intergranular fracture. This is best seen in viewgraph C13. Here, fractographs representative of the under, peak, and over aged conditions are presented. Fracture in each case is intergranular. The magnesium bearing alloy too deforms by localized slip. However, large, closely-spaced grain boundary precipitates are present in the microstructure due to the magnesium addition. The coarse grain boundary precipitates reduce the cohesive strength of grain boundaries. A condition is reached where stresses generated at the tip of the slip bands during deformation become sufficient to cause grain boundary decohesion in preference to slip plane decohesion, and intergranular fracture results. This is thought to be the primary reason why the ductility for the overaged condition of the Al-Li-Cu-Mg alloy remains low.

Microstructural Instability

In order to minimize the loss of material associated with specimen fabrication, the Al-Li-Cu alloys were hot rolled to 1.5 mm thick strip. The strip was hot rolled at about 700 K (427°C) with rolls maintained at 450 K(170°C). The section thickness was reduced about 5% per pass, and the material was reheated to 700°K after every four passes. The hot rolled strip was then solution heat treated and quenched in preparation for specimen fabrication. This processing resulted in microstructural instability in the magnesium bearing alloy, and this is the subject of the following discussion. In viewgraph VG C15, the tensile strength of the hot rolled and as extruded conditions are compared for both alloys. In VG C16 thru VG C18, microsctructural changes are documented.

In VG C15, the variation in tensile strength of the base and magnesium bearing alloys is compared for the hot rolled vs. extruded conditions. The properties of Al-Li-Cu-Mg represent

463K(190°C) aging and are presented on the left portion of the viewgraph. The base alloy properties are compared for 443K(170°C) aging and the respective trend curves are to the right of center.

The following are observed:

(1) There is an approximate strength decrement of 180 MPa (26 Ksi) for the hot rolled Al-Li-Cu-Mg when compared to the as-extruded condition at any given aging time.

(2) There is an approximate 60 MPa (8.5 Ksi) strength decrement for the hot rolled Al-Li-Cu alloy when compared to the as-extruded condition irrespective of aging time.

These are rather substantial reductions in strength, particularly in the case of the magnesium bearing alloy. Note also that the strength decrement is uniform over a broad range of aging conditions.

The microstructure of the extruded plate for the base (upper) and magnesium bearing (lower) alloys is represented in VG C16 for longitudinal sections. That is, the extrusion direction (E.D.) is from left to right (on the horizontal) in this viewgraph. Columnar grains. elongated in the extrusion direction and bounded by rows of zironium particles, characterize both microstructures. Recrystallization has occured in both alloys, and the distribution of zironium particles has effectively restrained grain growth.

The microstructure of the hot rolled strip for the Al-Li-Cu alloy is represented in the micrographs of VG C17. Here, the rolling direction (R.D.) is from left to right (on the horizontal) in the upper (longitudinal section) micrograph, and normal to the plane of the paper in the lower (transverse section) micrograph. A fine, laminated grain structure is observed in the longitudinal section. Equiaxed and uniformly fine grains

are present in the lower (transverse) micrograph. Large (60 μm long) particles, such as that in the upper micrograph of VG C17, are present in both aluminum-lithium-copper alloys. Energy dispersive analysis indicates the particles do not contain Zr, Mg, or other trace elements.* The particles may relate to the master alloy addition and are probably carry-overs from the melt during the atomization process. The point of fracture initiation in approximately 10% of the tensile tests was associated with such particles.

The microstructure of the hot rolled strip for the Al-Li-Cu-Mg alloy is represented in the micrographs of VG C18. Longitudinal and transverse orientations are presented. Extensive recrystallization and grain growth are observed in the magnesium containing alloy. The microstructure consists of large grains (greater than 100 μm in diameter) amongst local clusters of small, equiaxed grains. Coarse precipitates are observed along grain boundaries.

Recrystallization and grain growth in the Al-Li-Cu-Mg alloy may explain a component of the 180 MPa strength decrement between the hot rolled and as-extruded conditions. However the magnitude of the effect in the magnesium bearing alloy and the fact that a significant decrement occurs in the Al-Li-Cu suggest a second contribution. The hot rolling process apparently results in either (1) less solute being available for transformation to δ' (and/or θ'), or (2) much more heterogeneous precipitation. Specimens to assess the degree of Li and/or Mg loss as a result of the hot rolling process have been analyzed and the data indicate little or no loss of lithium (and/or Mg in the case of the magnesium bearing alloy) occurs as a result of hot rolling. Transmission electron microscopy (TEM) of thin film specimens is in progress, and this may contribute to an understanding of this anomalous behavior.

---

* The energy dispersive system available could not detect the presence of low atomic number elemental spectrum such as that of Li.

SUMMARY

The mechanical properties and microstructural evaluation of the two reference Al-Li-Cu alloys is summarized in VG C19. The following are concluded:

(1) Both the base and the magnesium bearing alloys exhibit high strength but limited ductility

(2) The addition of magnesium to the base alloy increases the tensile strength, has little affect on ductility, changes the fracture mode from non-ductile shear to intergranular fracture over a broad range of aging conditions, and changes the fracture profile from shear to tensile (or load normal) fracture.

(3) Under similar hot rolling conditions, the magnesium bearing alloy exhibits substantial recrystallization and grain growth; more Zr is required to maintain a stable microstructure.

THE AGING RESPONSE OF TWO ALUMINUM-LITHIUM POWDER METALLURGY ALLOYS

PATRICK P. PIZZO
Advanced Research and Applications Corporation

HOWARD G. NELSON
NASA-Ames Research Center

WORK SPONSORED UNDER NASA CONTRACT NAS-10365

VG C1

OVERVIEW

- DESCRIBE THE TWO Al-Li-Cu ALLOYS
  - COMPOSITION
  - P/M PROCESSING STEPS
- COMPARE THE ALLOYS IN TERMS OF:
  - AGE HARDENING
  - STRENGTHENING
  - DUCTILITY

  } CHARACTERISTICS
- COMPARE THE FRACTURE CHARACTERISTICS
- DEMONSTRATE A DIFFERENCE IN MICROSTRUCTURAL STABILITY FOR HOT ROLLED SHEET

VG C2

ALUMINUM-LITHIUM ALLOYS INVESTIGATED

BASE ALLOY: Al-2.6% Li-1.4% Cu

MAGNESIUM BEARING ALLOY: Al-2.6% Li-1.4% Cu-1.6% Mg

VG C3

P/M PROCESSING STEPS

- POWDERS PRODUCED BY QUICKLY COOLING AN ATOMIZED MOLTEN STREAM OF THE Al-Li-Cu ALLOYS IN AN ARGON ATMOSPHERE:
  - COOLING RATE ABOUT 10^3 C/S
  - SPHERICAL PARTICLES
  - PARTICLE DIAMETER ABOUT 150 μm
- POWDERS PACKED IN A 6061 ALUMINUM CAN AND ISOSTATIC PRESSED TO 415 MPa
- BILLET HOT UPSET AT 480°C; THEN EXTRUDED AT 400°C THROUGH A 2½ BY ½ INCH, ROUND CORNER DIE
  - MAXIMUM EXTRUSION RATIO OF ABOUT 10:1

VG C4

CHARACTERISTICS COMPARED:

- AGE HARDENING
- STRENGTHENING
  - YIELD STRESS (YS)
  - ULTIMATE TENSILE STRESS (UTS)
- DUCTILITY
  - AS MONITORED BY THE PLASTIC STRAIN-TO-FRACTURE, e_f

VG C5

AGING RESPONSE AS A FUNCTION OF AGING TIME: A COMPARISON

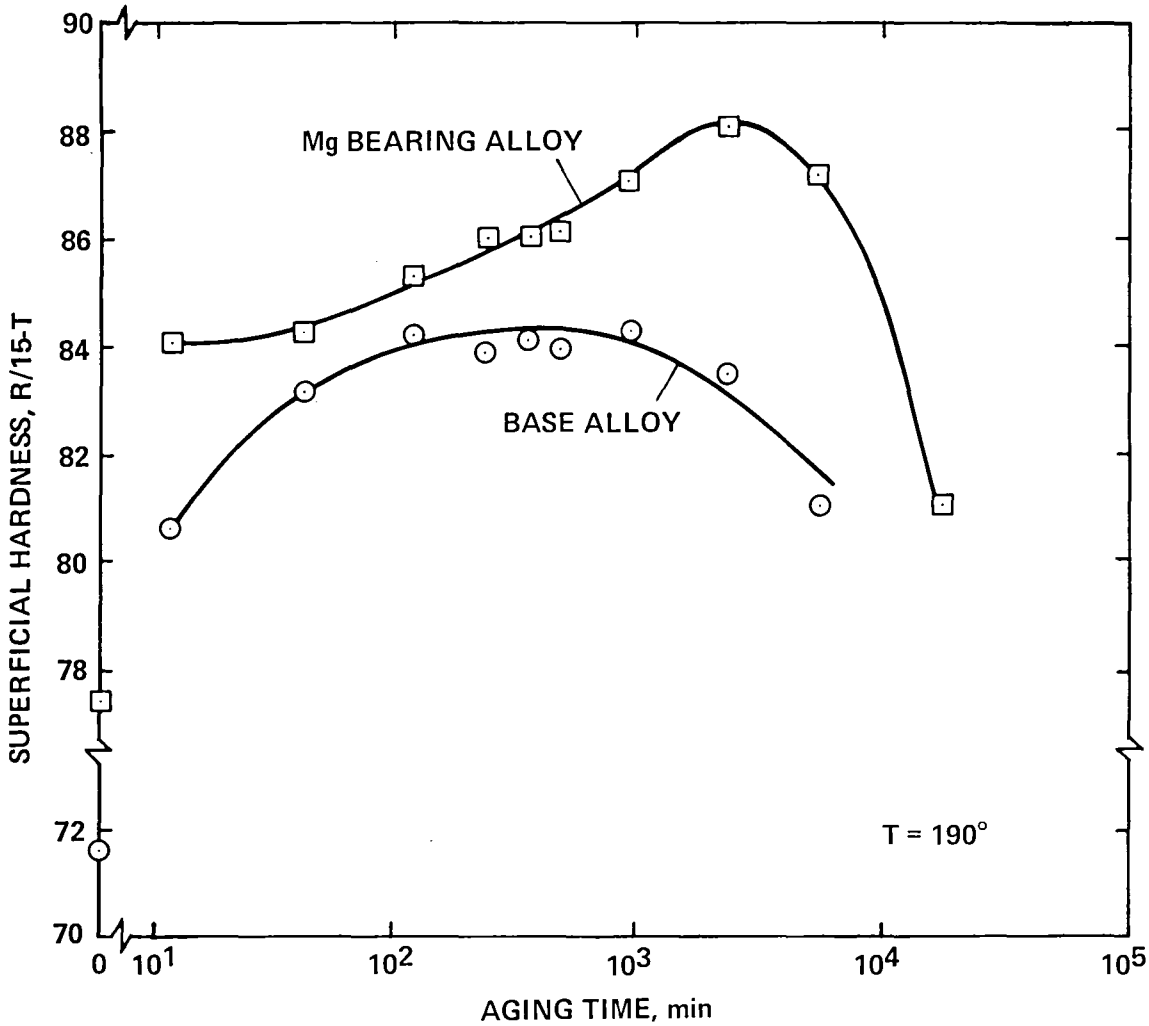

VG C6

STRENGTHENING CHARACTERISTICS:

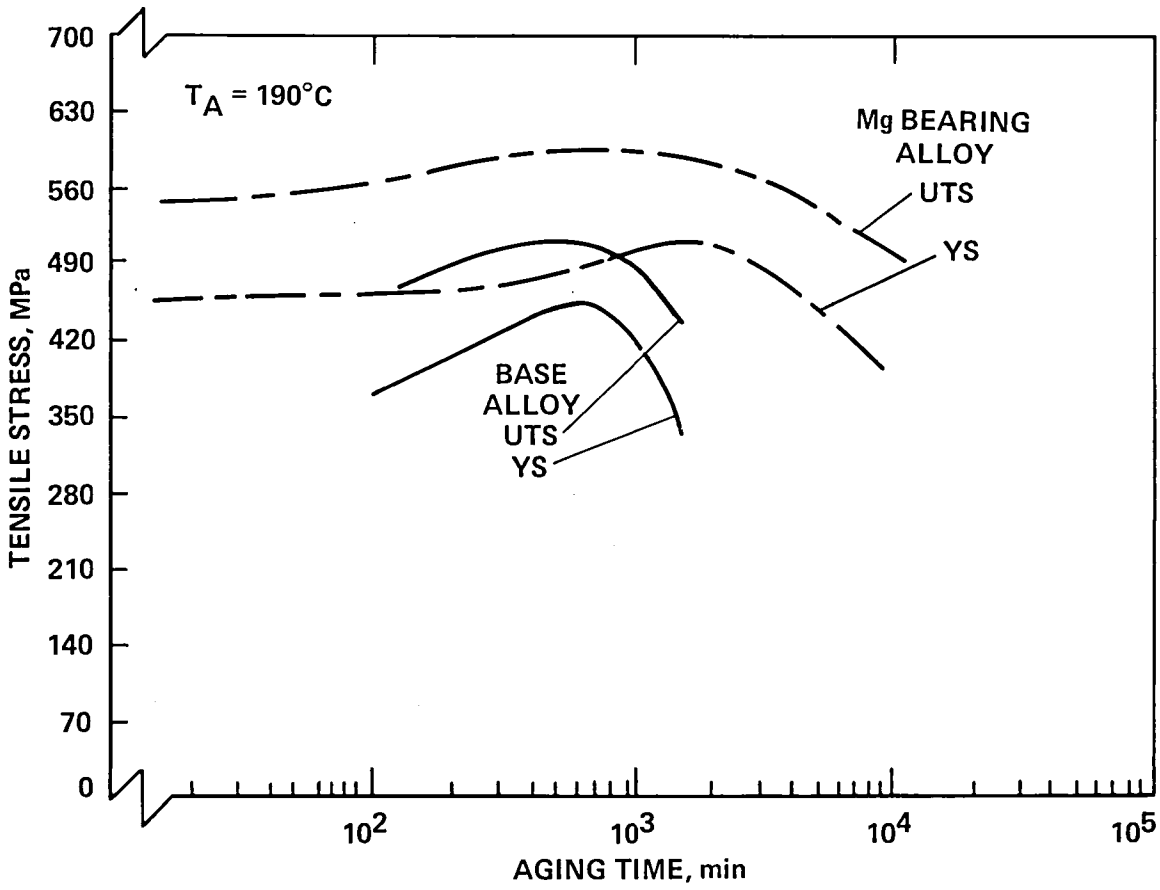

VG C7

PLASTIC STRAIN-TO-FRACTURE TREND CURVES

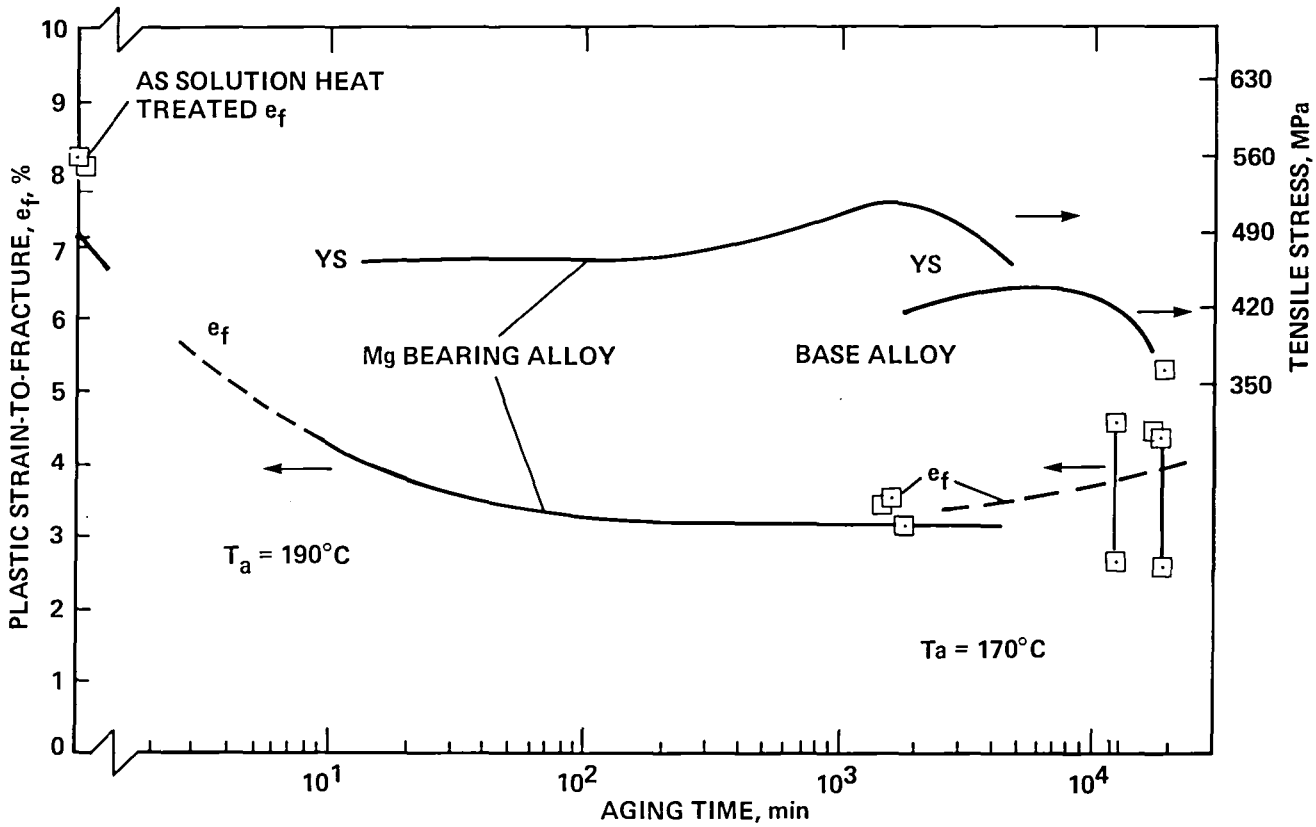

VG 88

TENSILE PROPERTIES AT PEAK STRENGTH

BASE ALLOY (Al-Li-Cu)		MAGNESIUM BEARING ALLOY (Al-Li-Cu-Mg)
550 MPa (80 Ksi)	UTS	600 MPa (87 Ksi)
460 MPa (67 Ksi)	YS	520 MPa (75 Ksi)
3.0%	e_f	~ 3.5%

NOTE:
- SPECIMENS EXHIBITED LIMITED REDUCTION IN AREA
- SERRATED FLOW WAS OBSERVED FOR THE Mg BEARING ALLOY AT EARLY AGING TIMES

VG C9

OBJECTIVE: COMPARE THE FRACTURE CHARACTERISTICS OF THE BASE AND Mg BEARING ALLOYS

VG C10

COMPARISON OF FRACTURE PROFILES

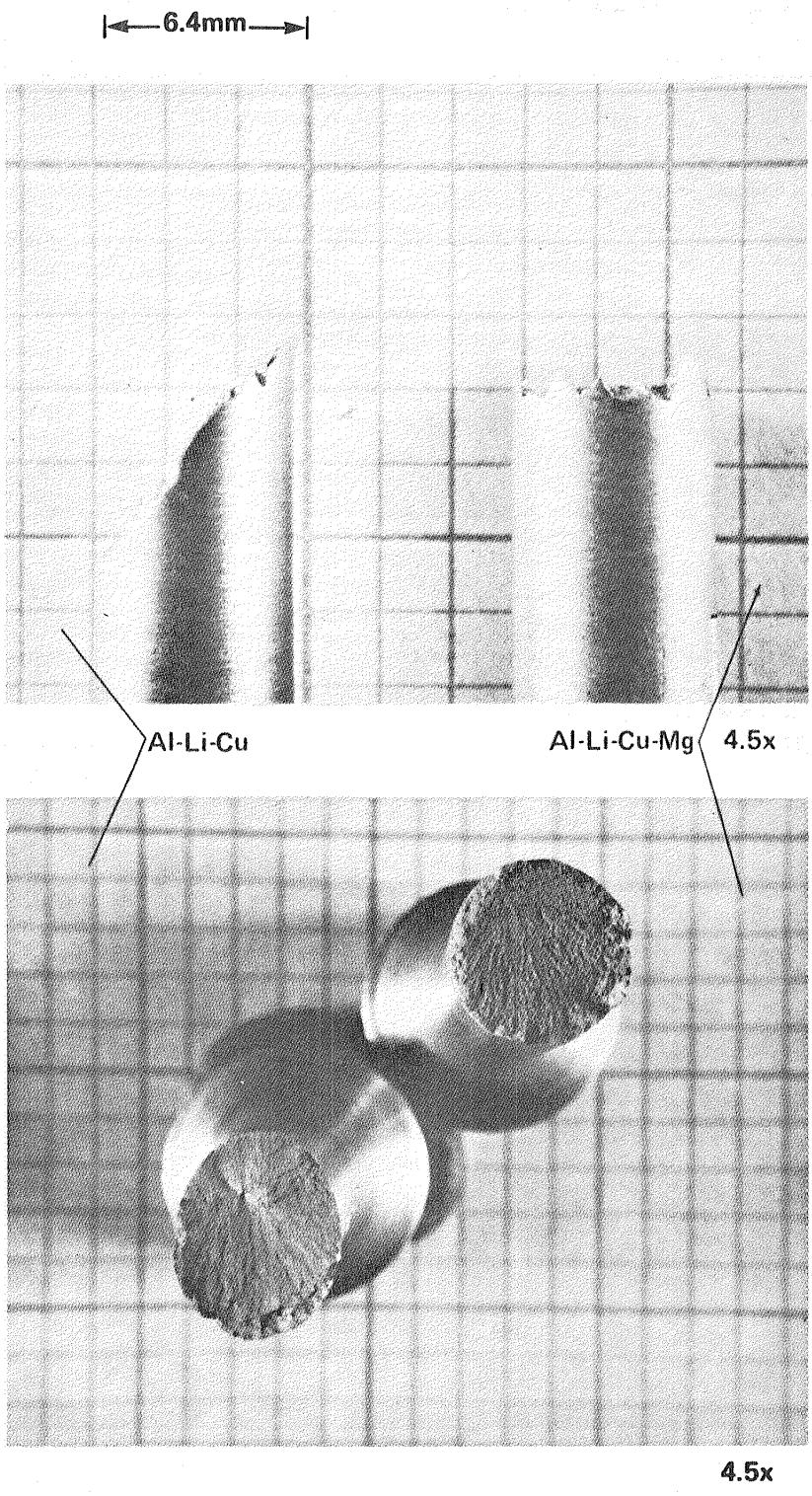

VG C11

COMPARISON OF FRACTURE MORPHOLOGY

Al-Li-Cu

20μm

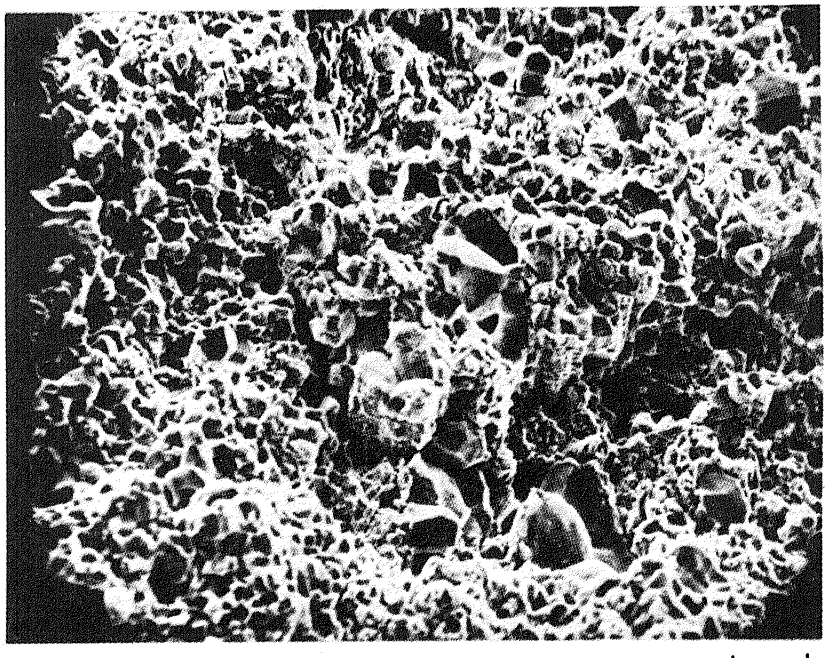

Al-Li-Cu-Mg

20μm

VG C12

AGING AND FRACTURE RESPONSE OF Al-Li-Cu-Mg

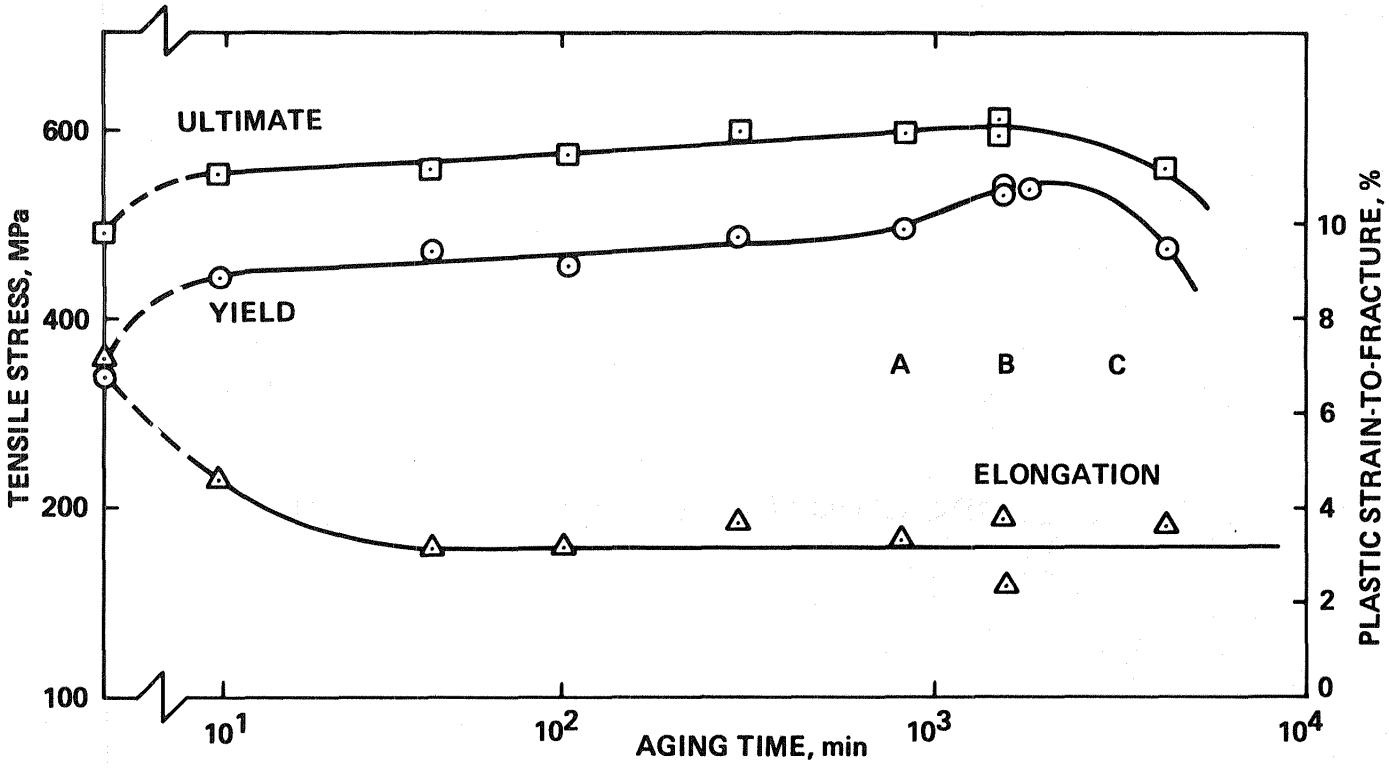

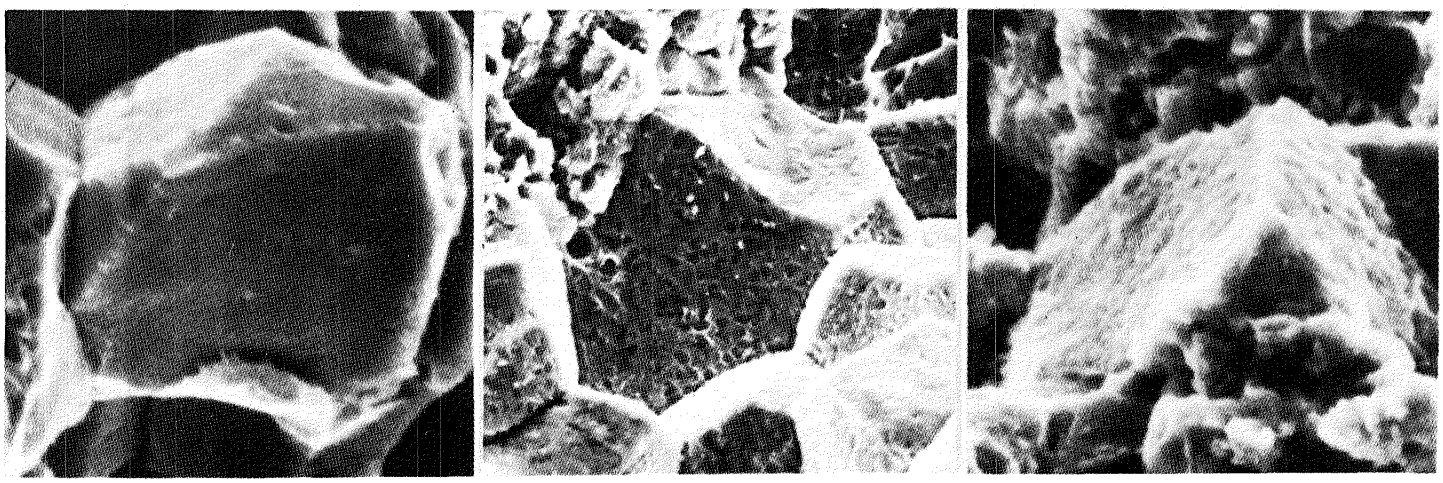

A 5μm B 5μm C 5μm

VG C13

A COMPARISON OF THE MICROSTRUCTURAL INSTABILITY IN RESPONSE TO HOT ROLLING

VG C14

THE EFFECT OF HOT-ROLLING ON THE TENSILE PROPERTIES

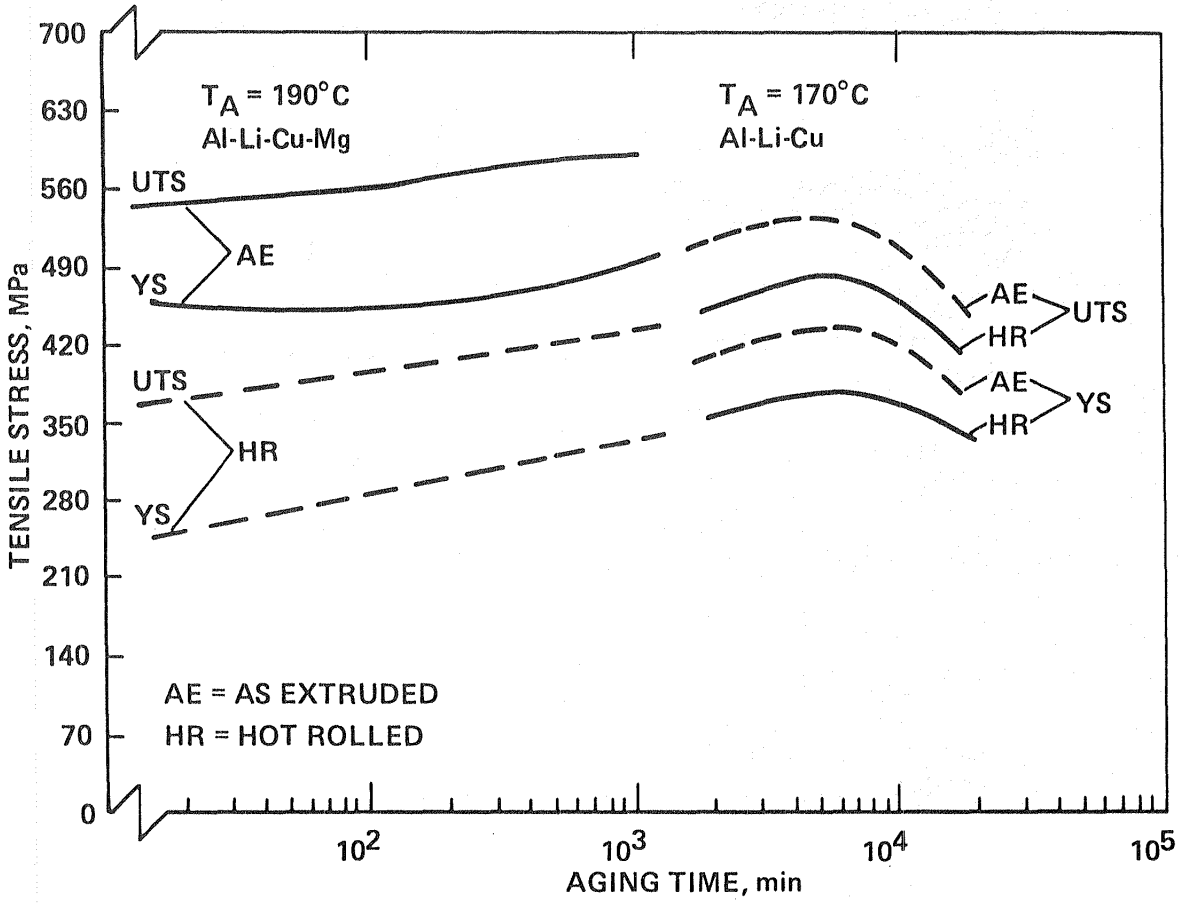

VG C15

MICROSTRUCTURE OF THE AS-EXTRUDED, SOLUTION HEAT TREATED AND PEAK AGED CONDITION

Al-Li-Cu

20μm

Al-Li-Cu-Mg

LONGITUDINAL

20μm

VG C16

MICROSTRUCTURE OF THE BASE ALLOY IN THE HOT ROLLED CONDITION

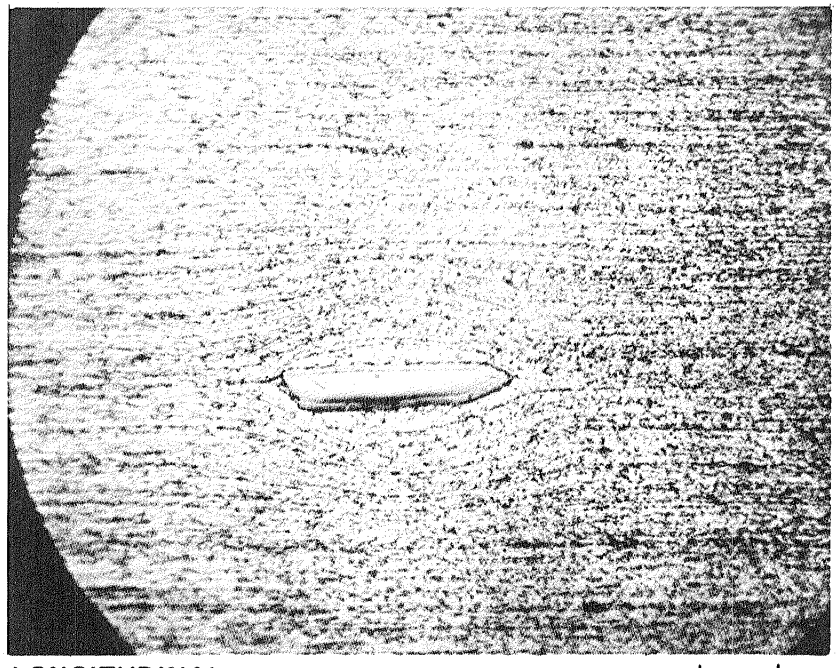

LONGITUDINAL

30μm

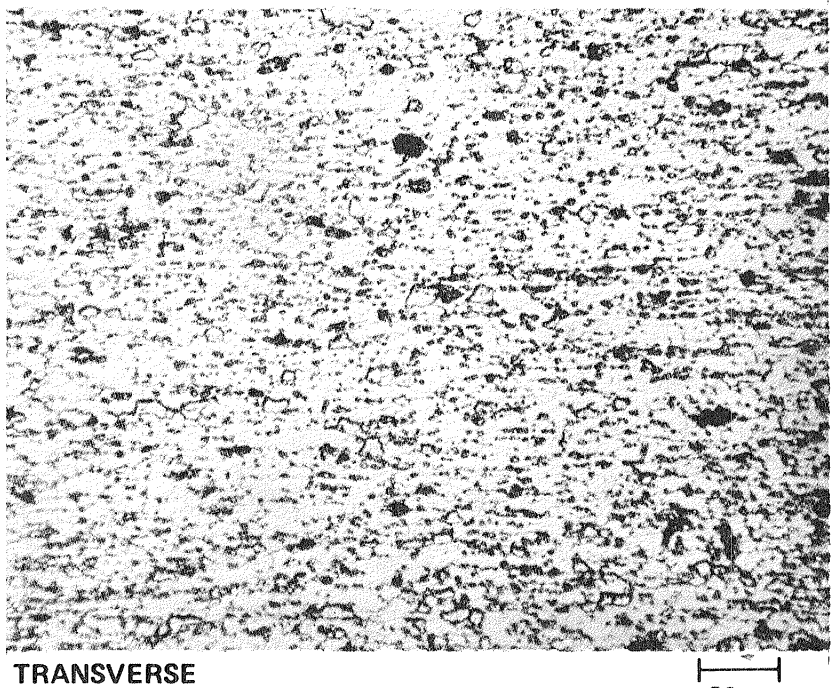

TRANSVERSE

20μm

VG C17

MICROSTRUCTURE OF THE MAGNESIUM BEARING ALLOY IN THE HOT ROLLED CONDITION

LONGITUDINAL

40μm

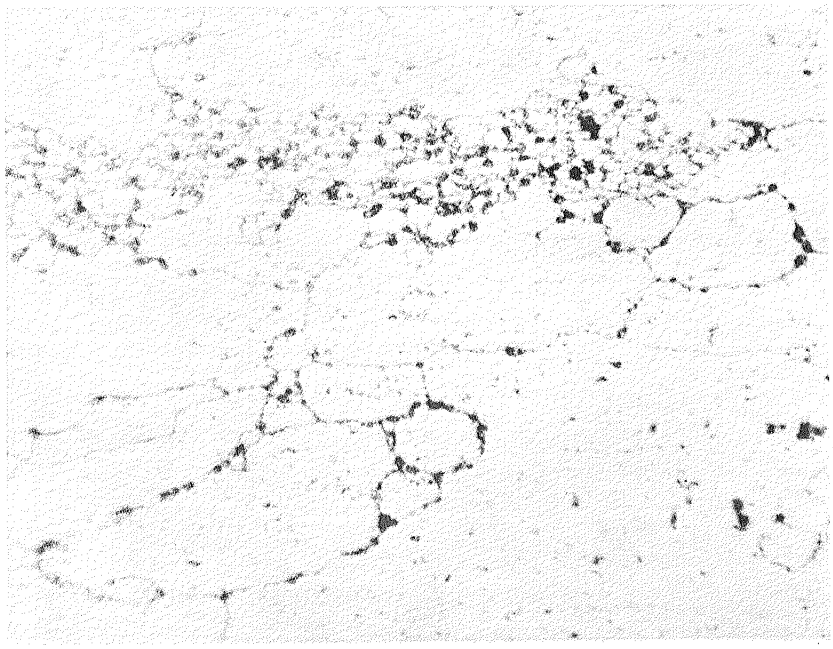

TRANSVERSE

20μm

VG C18

SUMMARY

1. BOTH COMPOSITIONS EXHIBIT HIGH STRENGTH, BUT LIMITED DUCTILITY

2. THE ADDITION OF Mg TO THE BASE ALLOY
   - INCREASES THE STRENGTH
   - DOES NOT AFFECT DUCTILITY
   - CHANGES THE FRACTURE MODE FROM NON-DUCTILE SHEAR TO INTERGRANULAR FRACTURE
   - CHANGES THE FRACTURE PROFILE FROM SHEAR TO TENSILE

3. UNDER SIMILAR HOT ROLLING CONDITIONS, THE Mg BEARING ALLOY EXHIBITS RECRYSTALLIZATION AND GRAIN GROWTH; MORE Zr IS REQUIRED TO MAINTAIN STABLE MICROSTRUCTURE

VG C19

Section D

THE TIME-TEMPERATURE PARAMETRIC ANALYSIS OF THE AGING RESPONSE OF ALUMINUM-LITHIUM-COPPER ALLOYS

BACKGROUND

In evaluating the aging response of the two reference aluminum-lithium-copper alloys, it was observed that although the kinetics for peak strengthening were more sluggish in the magnesium bearing alloy, the early age strengthening response was more rapid. Indeed, data reported in the first annual report indicate that significant hardening occurs in the Al-Li-Cu-Mg for a fixed aging time at relatively low aging temperatures (373K). The initial aging response is the subject of Section D. The data were obtained in the last contract period, and the results were reported at the Fall Meeting of TMS-AIME in Louisville, Kentucky (October 1981). The viewgraphs of that presentation will be used to document the aging study in this report.

LIST OF VIEWGRAPHS

OVERVIEW

The initial aging behavior of the two reference Al-Li-Cu alloys is the subject of this Section. The compositions of the two alloys are presented in VG D2. The alloys were produced using advanced powder metallurgical processing techniques. Interest in the initial aging response was stimulated by the data of VG D3 which were reported in the First Annual Report for NASA Contract NAS-10365. This viewgraph shows the age hardening characteristics of the base and the magnesium bearing alloys for a fixed aging time; the aging temperature is varied. Substantial hardening is observed for the alloy containing magnesium to relatively low aging temperatures (373K or 199°C). Data presented in Section C confirm that the rate of strengthening in the Al-Li-Cu-Mg alloy is initially rapid. Ninety percent of the value of peak strength is attained in the first 10 minutes of aging at 463 K(190°C). Peak strengthening is reached in about 1800 minutes at this aging temperature. A study of the initial age hardening response is presented herein.

Viewgraph D4 presents an overview of the aging study. It will be shown that the age hardening for both Al-Li-Cu alloys is linear on a semi-log plot of hardness versus the log of aging time. The base alloy exhibits a significant incubation time while the magnesium bearing alloy does not. The aging behavior of the base alloy is systematic over a broad range of temperature and the data are tractable using the time/temperature parametric approach of Manson and Haferd.* The aging behavior of the magnesium bearing alloy is complex and the initial hardening kinetics are very rapid.

---

* S.S. Manson and A.M. Haferd, NACA Tech. Note 2890, March, 1953; S.S. Manson, G. Succop, and W.R. Brown Jr., Trans. ASM, Vol. 51, pp. 911-934, 1959.

Age Hardening Characteristics

To scope the aging response of the two Al-Li-Cu alloys, hardness tests were performed on coupon specimens 12mm by 8mm by 1.5mm sectioned from hot rolled strip. The strip was hot rolled at about 700°K (427°C) with rolls maintained at 450 K (177°C). The section thickness was reduced about 5% per pass, and the material was reheated to 700 K (427°C) after every four passes. In this manner, a 1.5 mm thick strip was prepared from the 14.7 mm thick original extrusion. The Rockwell 15-T superficial hardness scale was used to measure hardness. Aging was performed in either a forced circulation oven or in a sand flotation bath. The aging temperature was maintained $\pm$ 2K. The aging time was measured from the time when the target temperature minus 2K was attained. This was determined from thermocouple output from an instrumented dummy sample concurrently exposed.

The linear age hardening behavior on a semi-log plot of hardness versus aging time is demonstrated in VG D5 for both alloys and for an aging temperature of 373K (100°C). The as solution heat treated hardness is indicated at zero aging time. Although both alloys exhibit the same slope;

$$t \frac{dH}{dt} = \alpha \quad \text{where } \alpha \text{ is a constant} \quad \text{Eq (1)}$$

the base alloy is characterized by a substantial incubation time, t_i with respect to the magnesium bearing alloy (about 15 minutes). A real time incubation period was noted for the base alloy over a broad range of aging temperature.

Aging trend lines for the Al-Li-Cu alloy for temperatures ranging from 85°C to 205°C are presented in VG D6. The as solution heat treated hardness is noted by the open data point at zero aging time and the dashed horizontal line. Saturation hardness is about 85 R/15-T. Incubation times (>1min) are

noted for aging temperatures through 135°C. Slopes are constant and aging lines appear to be systematically displaced to shorter aging times as the aging temperature is increased. A transition in behavior is observed for 170°C aging. At 170°C and for aging times in excess of 10 minutes, and at the higher aging temperatures, the slope of H vs. log t_A is decreased. Due to the systematic aging behavior of VG D6, the attempt was made to correlate the data using the time/temperature superposition method of Manson and Haferd.

The Manson-Haferd Time/Temperature Parameter

The Manson-Haferd parametric technique is a empirical method of correlating elevated temperature mechanical properties data such as creep rate and stress rupture data in terms of time and temperature. In order to apply the techinque to the data of VG D6, the data were cross plotted. That is, the data of VG DG were used to generate a cross-plot of the log of the aging time as a function of aging temperature for constant hardness: VG D7. Data thru 135°C have been included in the analysis. Where necessary, the trend lines of VG D6 were extrapolated to determine the aging time to achieve a given hardness.

The lines of VG D7 appear parallel. But the method of Manson-Haferd assume that the lines intersect at a common point. This is illustrated in VG D8. The Manson-Haferd correlation paremeter P_{M-H}, is given by:

$$P_{M-H} = \frac{\text{Log } t - \log t_a}{T - T_a} \qquad \text{Eq (2)}$$

where T_A and t_a are the respective coordinates of the common intercept. The data of VG D7 were fit using linear regression analysis, and a common intercept resulted.

The respective values of Ta and t_a were inserted in equation(2), and the raw hardness data were used to establish the trend lines of VG D6 were replotted as a function of the correlation parameter, P_{M-H}. These data are presented in VG D9. The Manson-Haferd parameter is observed to normalize the aging data of the base alloy over the broad range of aging times and temperatures investigated.

Although the Manson-Haferd method is empirical, the nearly parallel lines of VG D7 can be used to estimate the activation energy for the process active in determining the age hardenability of the Al-Li-Cu. From the slope of these data, an approximate activation energy of 26.2 kcal/mole (110 KJ/mode) is determined. This is in reasonable agreement with the value of 29.5 kcal/mode (124 KJ/mole) reported by Kamel, Ali and Farid in aging studies of Al-Li alloys.*

The Manson-Haferd parametric technique could not be applied in the analysis of the aging data for the magnesium bearing alloy because the age hardening did not vary systematically. This is seen in VG D10, where trend lines are presented for Al-Li-Cu-Mg for aging temperatures ranging from 75°C to 205°C. The as solution heat treated hardness is indicated at zero time by the open data and by the horizontal dashed line. Note that both the slope and y-intercept of the aging lines vary in an irregular fashion. The age hardening of Al-Li-Cu-Mg is found to be complex and not simply tractable using the Mason-Haferd parametric technique.

Note also in VG D10 that the initial age hardening of the magnesium bearing alloy is very rapid. At 185°C, the hardness jumps from 72 to 80 in about one minute. This rapid hardening may alternatively be viewed as the result of increasingly shorter incubation times with increasing temperature as the data are plotted on semi-log coordinates. Differential scanning calorimetric analysis and thin film TEM are currently in progress to determine the nature of the initial rapid rate of age hardening in the magnesium bearing alloy.

* R. Kamel, A.R. Ali, and Z. Farid, Phys, Stat. Sol. (a) 45, pg 419 (1978)

SUMMARY

Results are summarized in VG D11. The aging response of Al-Li-Cu is found to be systematic. This suggests that one age hardening mechanism is dominant. The activation energy for this mechanism is about 26.2 K cal/moke (110KJ/mole). The aging response is analytically tractable using the Manson-Haferd parametric techniques.

The addition of magnesium to Al-Li-Cu complicates the age hardening behavior. The age hardening characteristics are not systematic, and the initial age hardening kinetics are very rapid.

TIME-TEMPERATURE PARAMETRIC ANALYSIS OF THE AGING RESPONSE OF ALUMINUM-LITHIUM ALLOYS

PATRICK P. PIZZO
Advanced Research and Applications Corporation

PAUL DAVIES-WHITE and H. G. NELSON
NASA-Ames Research Center

WORK SPONSORED UNDER NASA CONTRACT NAS-10365

VG D1

Al-Li ALLOYS INVESTIGATED

BASE ALLOY: Al-2.6% Li-1.4% Cu

MAGNESIUM BEARING ALLOY: Al-2.6% Li-1.4% Cu-1.6% Mg

VG D2

AGING RESPONSE AS A FUNCTION OF TEMPERATURE FOR 16h

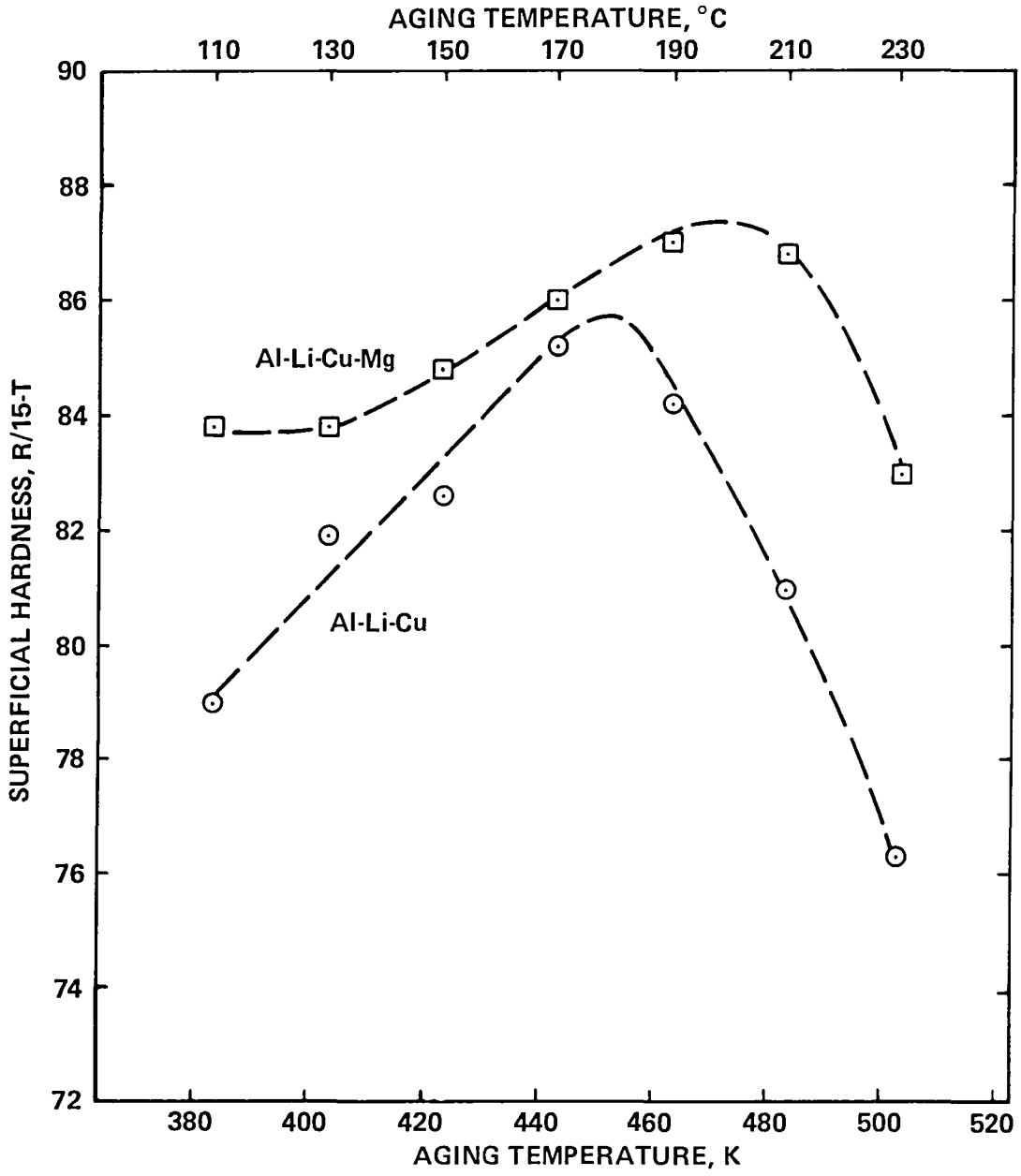

OVERVIEW

- LINEAR AGING BEHAVIOR IS OBSERVED FOR BOTH Al-Li-Cu ALLOYS ON A SEMI-LOG PLOT:

  H vs log ta

- THE BASE ALLOY (Al-Li-Cu) EXHIBITS A SIGNIFICANT INCUBATION TIME: THE MAGNESIUM BEARING ALLOY DOES NOT

- THE AGING BEHAVIOR OF THE BASE ALLOY IS SYSTEMATIC OVER A BROAD RANGE OF TEMPERATURE AND MATHEMATICALLY TRACTABLE

- THE AGING BEHAVIOR OF THE MAGNESIUM BEARING ALLOY IS COMPLEX: THE INITIAL HARDENING KINETICS ARE VERY RAPID

VG D4

AGING BEHAVIOR COMPARISON

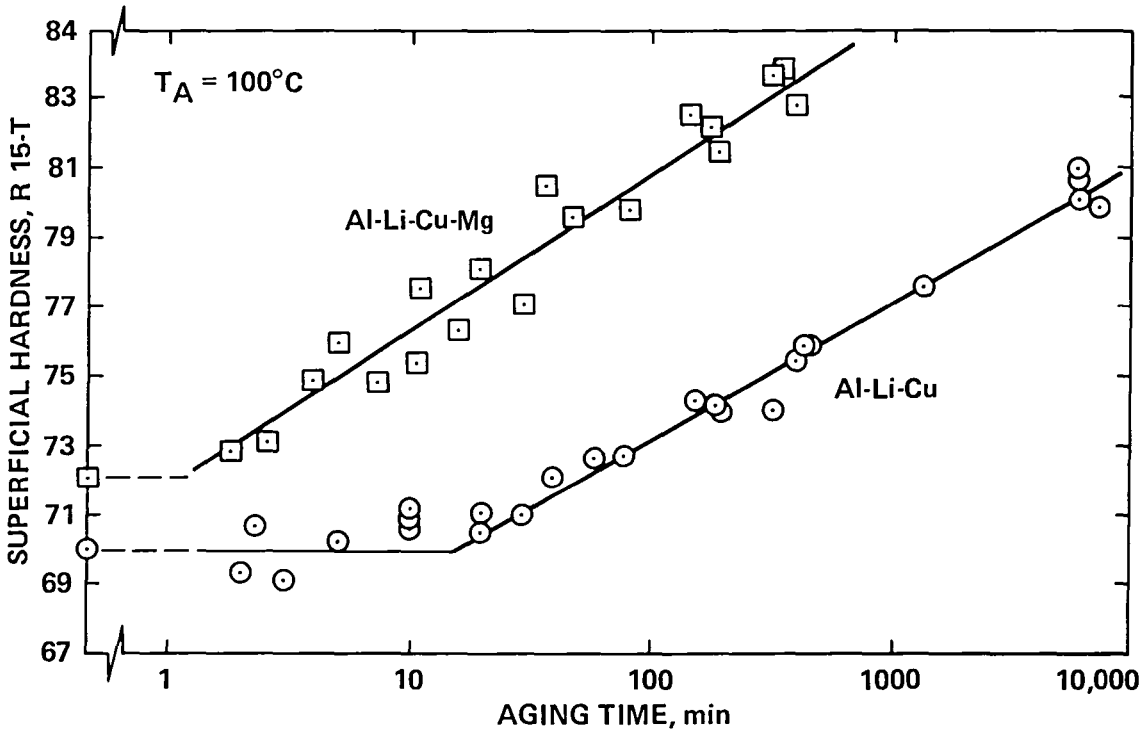

VG D5

AGING TREND OF THE BASE ALLOY

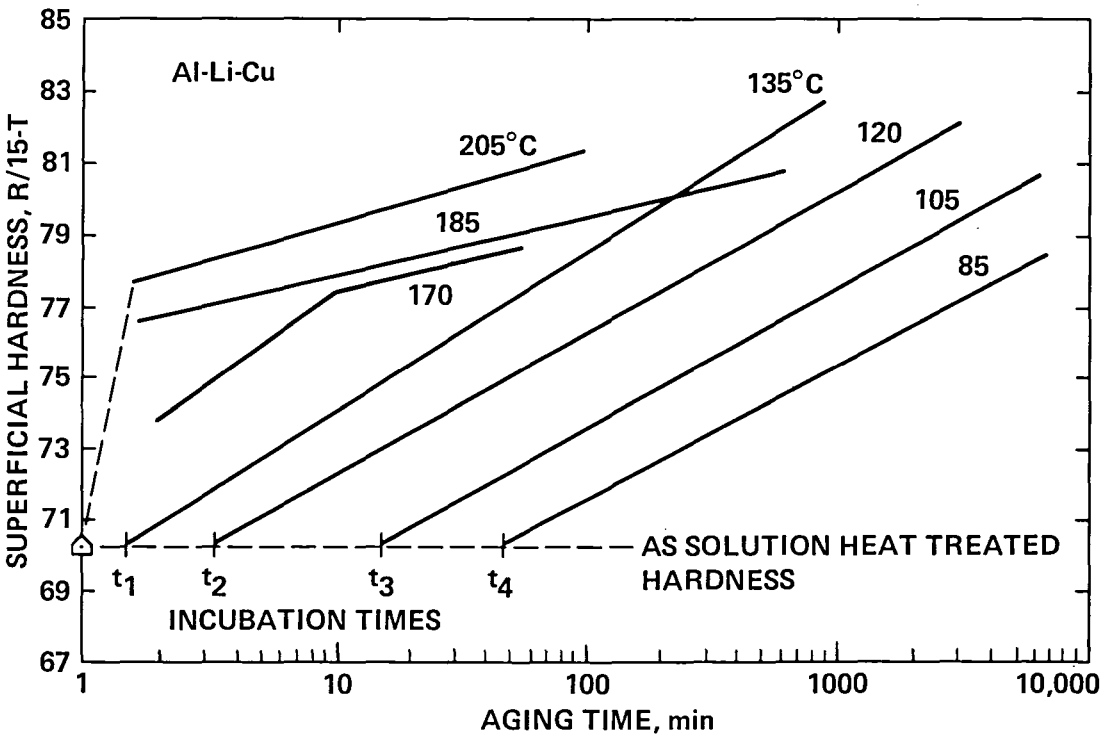

VG D6

TIME TO ACHIEVE A GIVEN HARDNESS AS A FUNCTION OF THE AGING TEMPERATURE

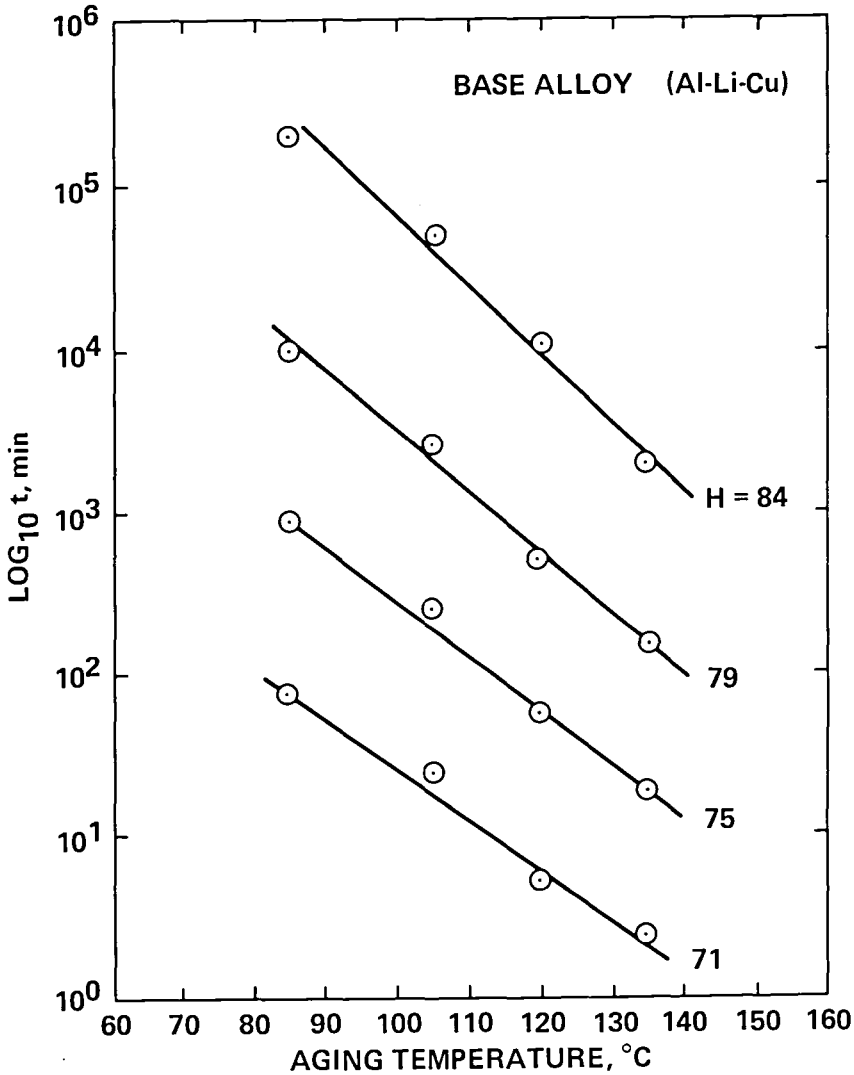

VG D7

MANSON-HAFERD
TIME/TEMPERATURE PARAMETER

$H = H(P)$

WHERE $P_{M\text{-}H} = \dfrac{\text{Log } t - \text{Log } t_a}{T - T_a}$

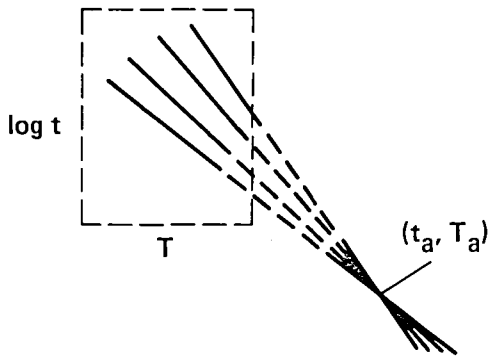

VG D8

AGING DATA NORMALIZED BY THE MANSON-HAFERD PARAMERIC TECHNIQUE

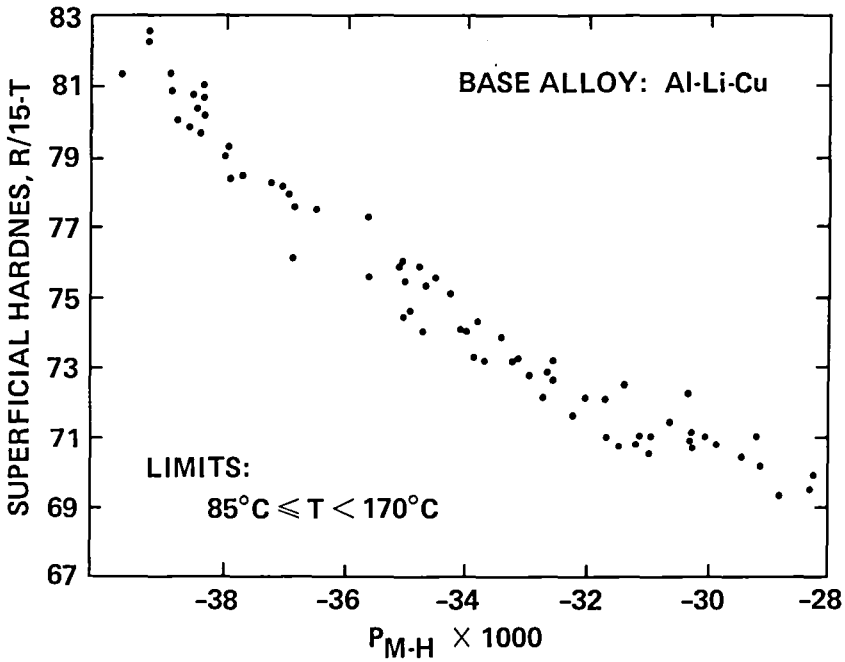

VG D9

THE AGING OF THE MAGNESIUM BEARING ALLOY

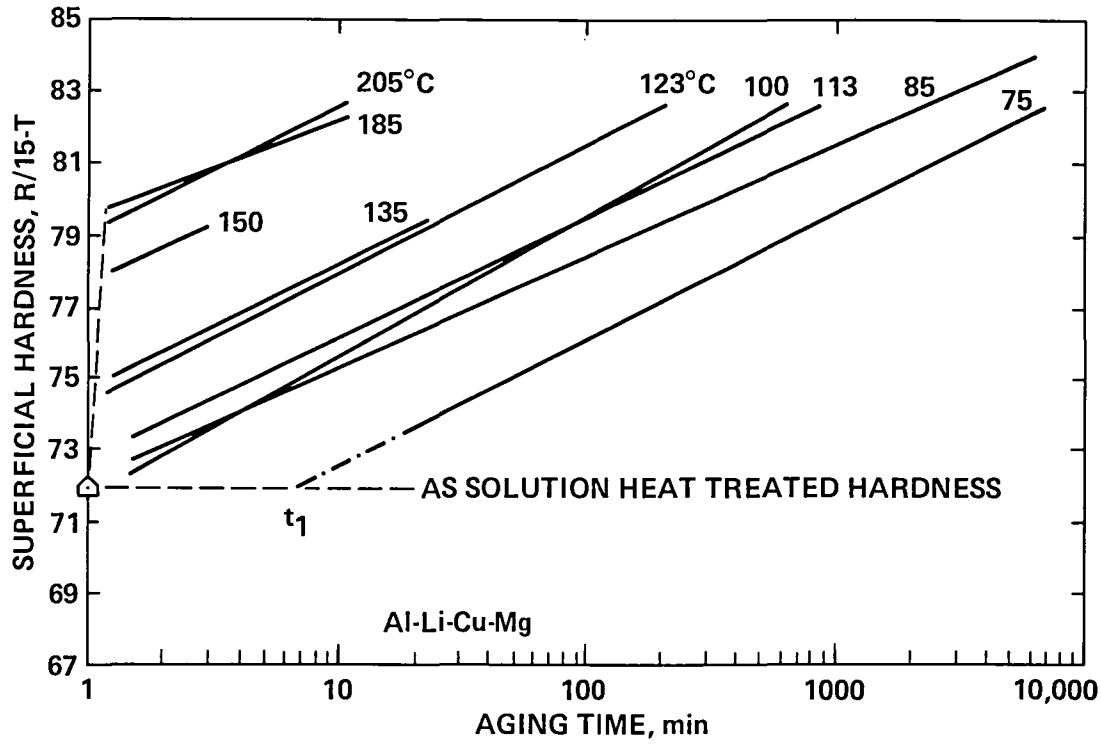

VG D10

SUMMARY

- AGING RESPONSE OF (Al-Li-Cu) IS SYSTEMATIC. THIS SUGGESTS THAT ONE HARDENING MECHANISM IS DOMINANT
- AGING RESPONSE IS MATHEMATICALLY TRACTABLE USING THE MANSON-HAFERD PARAMETER
- ADDITION OF MAGNESIUM TO THE BASE ALLOY COMPLICATES MODELLING THE BEHAVIOR
- INITIAL HARDENING KINETICS OF THE MAGNESIUM BEARING ALLOY ARE VERY RAPID

VG D11

RECAPITULATION

This report is a summary of the work completed in support of NASA Contract NAS-10365 during the contract period September 19, 1980 to September 18, 1981. As this is also the final report in that the principal investigator, Dr. Patrick P. Pizzo, has changed affiliation to San Jose State University, these data have been integrated with the tensile properties data submitted in the first annual report, ARACOR TR-45-1 dated September 1980, to form a comprehensive characterization of the two reference Al-Li-Cu alloys. In addition, the preliminary stress corrosion test results are also included. As the project was originally envisioned to be an approximate three year effort, the project, is at termination, on schedule. Stress corrosion screening tests have been completed and a statement regarding the relative stress corrosion resistance at Al-Li-Cu alloys has been issued.

The various SCC evaluation methods selected upon project inception are ample toward meeting the primary project objective which is to establish a practical stress corrosion screening technique for advanced aluminum alloy implementation. Perhaps the most significant contribution to be made shall be the selection of test specimens and methods which will allow accurate assessment of the SCC behavior of relatively brittle (low fracture toughness) but advanced metallic alloys. Efforts toward this goal are continuing in a concurrent research project thru NASA-AMES Research Center and San Jose State University, and the foundation of that research are the results reported herein. This completes evaluation of Al-Li-Cu alloys under Contract NAS-10365, "The Relative STress-Corrosion-Cracking Susceptibility of Candidate Aluminum-Lithium Alloys for Aerospace Structural Applications."

1. Report No.	2. Government Accession No.	3. Recipient's Catalog No.
NASA CR-3578		

4. Title and Subtitle	5. Report Date
THE RELATIVE STRESS-CORROSION-CRACKING SUSCEPTIBILTY OF CANDIDATE ALUMINUM-LITHIUM ALLOYS FOR AEROSPACE APPLICATIONS	June 1982
	6. Performing Organization Code
7. Author(s) Patrick P. Pizzo	8. Performing Organization Report No. TR-45-2
	10. Work Unit No. T-4241
9. Performing Organization Name and Address Advanced Research and Applications Corporation 1223 E. Arques Avenue Sunnyvale, California 94086	11. Contract or Grant No. NAS2-10365
	13. Type of Report and Period Covered Contractor Report
12. Sponsoring Agency Name and Address National Aeronautics and Space Administration Washington, DC 20546	14. Sponsoring Agency Code 505-33-21

15. Supplementary Notes Final Report

Ames technical monitor: Howard G. Nelson, 230-4, NASA Ames Research Center, Moffett Field, CA 94035, (415) 965-6137/FTS 448-6137

16. Abstract

The results of a two year study of Al-Li-Cu powder metallurgy alloys are summarized. Alloys investigated were Al-2.6%Li-1.4%Cu and Al-2.6%Li-1.4%Cu-1.6%Mg. The primary objectives of the study were to 1) identify a practical stress corrosion screening technique and 2) evaluate the relative stress corrosion crack resistance of these advanced Al-Li alloys. Much of the initial effort was involved in characterizing the base properties of the alloys. Processing, heat treatment, and size/orientation effects on the tensile and fracture behavior are established. Metallurgical and electrochemical conditions are identified which provide reproducible and controlled parameters for stress corrosion evaluation.

The preliminary stress corrosion test results are reported here. In smooth specimens designed primarily to monitor crack initiation, both Al-Li-Cu alloys were found to be more susceptible to stress corrosion crack initiation in an alternate immersion, aqueous sodium chloride environment than 7075-T6 aluminum. Only limited crack growth has been observed in bolt loaded DCB-type specimens. It is believed that general corrosion is obscuring stress corrosion cracking through crack tip blunting.

17. Key Words (Suggested by Author(s))	18. Distribution Statement
P/M alloys, Advanced Al-Li alloys, Aqueous chloride stress corrosion, Crack initiation, Crack growth.	Unlimited - Unclassified Subject Category - 26

19. Security Classif. (of this report)	20. Security Classif. (of this page)	21. No. of Pages	22. Price*
Unclassified	Unclassified	126	A07

*For sale by the National Technical Information Service, Springfield, Virginia 22161

NASA-Langley, 1982

End of Document